Elucidating the Diagnostic Potential of miRNA through Regulation of *Bcl-2* Apoptotic signaling nexus in Myocardial Infarction

By
Syed Hamid Abbas

Department of Biochemistry
Faculty of Biological Sciences
Quaid-i-Azam University
Islamabad, Pakistan
2023

Elucidating the Diagnostic Potential of miRNA through Regulation of *Bcl-2* Apoptotic signaling nexus in Myocardial Infarction

A dissertation submitted in the fulfillment of requirements for the

Degree of Master of Philosophy In Biochemistry/ Molecular Biology

By
Syed Hamid Abbas

Department of Biochemistry
Faculty of Biological Sciences
Quaid-i-Azam University
Islamabad, Pakistan
2023

Quaid-i-Azam University, Islamabad, PAKISTAN
Department of Biochemistry
Faculty of Biological Sciences

CERTIFICATE

This thesis, submitted by **Mr. Syed Hamid Abbas** to the Department of Biochemistry, Faculty of Biological Sciences, Quaid-i-Azam University, Islamabad, Pakistan, is accepted in its present form as satisfying the thesis requirement for the Degree of Master of Philosophy in Biochemistry/Molecular Biology.

Examination Committee:

1. **External Examiner:**
   Dr. Sumaira Farrakh
   Associate Professor
   Department of Bioscience,
   COMSATS, University Islamabad
   Signature: _____

2. **Supervisor:**
   Prof. Dr. Iram Murtaza
   Signature: _____

3. **Chairperson:**
   Prof. Dr. Iram Murtaza
   Signature: _____

Dated: **November 02, 2023**

DECLARATION

By submitting this thesis, I hereby declare that the entirety of the work contained therein is my own effort and hard work, that I am the authorship owner thereof and that I have not previously submitted it for obtaining any qualification.

Syed Hamid Abbas

This thesis is dedicated to my parents.

For their endless love, support, and encouragement

ACKNOWLEDGEMENT

All praises and thanks to Allah ﷻ, The Lord of the universe, The Most Beneficent and The Merciful, who showered His countless blessings upon us and helped me to contribute in the field of knowledge and enabled me to compile my humble endeavors in the shape of this thesis. Countless salutations upon The Holy Prophet, Hazrat Muhammad ﷺ, who is the source of knowledge and guidance for the entire humanity.

I would like to pay my sincere gratitude to my research supervisor and chairperson, Department of Biochemistry, **Dr. Iram Murtaza**, for giving me the opportunity to do my research under her supervision. Her keen interest, encouragement, dedication, guidance and scholarly advice throughout this research helped me to achieve my goal.

It is a genuine pleasure to express my deep sense of thanks and gratitude to my guide, **Ma'am Ayesha Ishtiaq**. Her scientific approach, timely advice and overwhelming attitude to guide me was mainly responsible for completing my work. I would also like to thank my senior, **Sir Khadim Hussain,** for supporting and helping.me. I would also like to thank my cooperative lab members and staff.

I am most indebted to my **Parents** and siblings **S. Ali Abbas**, **S**. **Atta Hussain**, **S.M. Hadi** and my dearest **S. Abdus Saleh** for their endless prayers, matchless love, and care. Words become meaningless when I have to say thanks to them; their prayers gave me strength and hope to accomplish this task and to pursue my goals.


بسم الله الرحمن الرحيم

TABLE OF CONENTS

LIST OF ABBREVIATIONS

CAD	Coronary artery disease
M	Myocardial infarction
ALT	Alanine Aminotransferase
AMI	Acute Myocardial Infarction
ANP	Atrial Natriuretic Peptide
AP1	Activating Protein
APAF-1	Apoptotic Protease Activating Factor-1
APS	Ammonium Persulphate
APX	Ascorbate Peroxidase
AST	Aspartate Aminotransferase
ATP	Adenosine Triphosphate
BCIP	5-Bromo-4-Chloro-3-Indolylphosphate
BCL-2	B cell lymphoma 2
BNP	Brain Natriuretic Peptide
BSA	Bovine Serum Albumin
BAX	*BCL-2* associated X protein
CAD	Coronary Artery Disease
cAMP	Cyclic Adenosine Monophosphate
CAT	Catalase
CK-MB	Creatine Kinase Myocardial Band
CRP	C-Reactive Protein
cTn	Cardiac Troponin
CVDs	Cardiovascular Diseases
cyt c	Cytochrome Complex
DAG	Diacylglycerol
DNA	Deoxyribonucleic Acid

dNTPs	Deoxynucleotide Triphosphates
DRP-1	Dynamin receptor 1
ECG	Electrocardiogram
EDTA	Ethylene diamine tetraacetic acid
ER	Endoplasmic Reticulum
ERK	Extracellular Signal Regulated Kinase
ET-1	Endothelin-1
EVs	Extracellular Vesicles
$FeSO_4$	Ferrous Sulphate
GDP	Guanosine Diphosphate
GPCR	G-Protein Coupled Receptor
GSH	Reduced Glutathione
GTP	Guanosine Triphosphate
H&E	Hematoxylin and Eosin
H_2O_2	Hydrogen Peroxide
HDL	High-Density Lipoprotein
I/R	Ischemia/Reperfusion
IP3	Inositol Trisphosphate
ISO	Isoproterenol
JNK	Jun N-terminal Kinases
LDH	Lactate Dehydrogenase
LDL	Low-Density Lipoprotein
MAPK	Mitogen Activated Protein Kinase
MAPKK	Mitogen Activated Protein Kinase Kinase
MAPKKK	Mitogen Activated Protein Kinase Kinase Kinase
MDA	Malondialdehyde
MDH	Malate Dehydrogenase

MDHA	Mono-Dehydroascorbic Acid
MI	Myocardial Infarction
miRNA	MircoRNA
MOMP	Mitochondrial Outer Membrane Permeability Pore
MPTP	Mitochondrial Permeability Transition Pore
MRI	Magnetic Resonance Imaging
mRNA	Messenger RNA
NaCl	Sodium Chloride
NBT	Nitro-Blue Tetrazolium
NC	Nitrocellulose
NFATC3	Nuclear Factor of Activated T-Cells Cytoplasmic 3
NIH	National Institute of Health
PCR	Polymerase Chain Reaction
PIP2	Phosphatidylinositol 4,5-Bisphophate
PKA	Protein Kinase A
PKC	Protein Kinase C
PLC	Phospholipase
PMSF	Phenyl Methylsulfonyl Fluoride
POD	Peroxidase
pre-miRNA	Precursor miRNAs
pri-miRNA	Primary miRNAs
RIPA	Radio Immune Precipitation Assay
RISC	RNA-Induced Silencing Complex
RNA	Ribonucleic acid
ROS	Reactive Oxygen Species
RT-qPCR	Real Time-quantitative Polymerase Chain Reaction
SDS	Sodium Dodecyl Sulfate

SNS	Sympathetic Nervous System
SOD	Super Oxide Dismutase
STEMI	ST Elevation Myocardial Infarction
TBA	Thiobarbituric Acid
TBARs	Thiobarbituric Acid Reactive Substances
TBST	Tris Buffered Saline With 0.1% Tween-20
TCA	Trichloroacetic Acid
TNB	5'-Thio-2-Nitrobenzoic Acid
TNF	Tumor Necrotic Factor
TRBP	Trans Activation Response RNA Binding Protein
UTR	Untranslated Region
WHO	World Health Organization

LIST OF FIGURES

ABSTRACT

Myocardial infarction accounts for highest number deaths worldwide. The plaque formation in coronary artery disease is major cause of myocardial infarction. Myocardial infarction is characterized by oxidative stress, ischemia, and apoptosis. Accumulated evidence indicates the importance of circulating miRNAs as diagnostic biomarkers in myocardial infarction. Therefore, the aim of the study is to determine the involvement of miRNAs in *Bcl-2* apoptotic pathway and to utilize miRNAs as potential diagnostic biomarkers for myocardial infarction. Whole blood samples of CAD patients were taken for qRT-PCR gene expression analysis. Rat model of myocardial infarction was established by giving Isoproterenol. Biochemical analysis of reactive oxygen species and antioxidant activity was measured. Lipid profiling included cholesterol, triglyceride, ALT, and AST level assessment in isoproterenol rat group. *Bcl-2* expression was significantly decreased. ET-1 expression was increased in MI patient's blood. miR-98-5p expression was significantly decreased and significant increase in miR-15a expression in patient's sample. Bax and Drp-1 protein expression in isoproterenol administered rat group was increasedwith high significance. NFATc3 levels were declined in MI patient's samples. ROS and TBARS levels were increased with subsequent decrease in antioxidant activities in isoproterenol rat groupcompared to normal. Lipid profile assays show an increase in cholesterol and triglyceride levels alongwith high AST and ALT activities in isoproterenol group as that of normal rat group. It is concluded that miRNAs can be utilized as a better diagnostic strategy for coronary artery diseasepatients including myocardial infarction.

1. INTRODUCTION

Myocardial infarction (MI) is one of the cardiovascular diseases that has caused a high number of deaths worldwide (Q. Zhang *et al*., 2022). MI commonly known as "heart attack" is the result of reduction of blood flow to the arteries because of atherosclerotic plaque or thrombus (Ojha & Dhamoon, 2021). Consequently, depriving the region of heart from oxygen supply causing ischemia and hypoxia which leads to the death of cardiomyocytes (Hermann, Xin, Bähr, Giebel, & Doeppner, 2022). Heart and blood vessels make up the cardiovascular system. Number of diseases arise from the disturbances in the normal functioning of cardiovascular system collectively called as CVDs (Lopez *et al*., 2022). Across the globe, the major contributorof all the deaths is cardiovascular disease. Among all the cardiovascular diseases, 49.2% deaths occurred due to ischemic heart disease in 2019 (Roth *et al*., 2020). Coronary artery disease (CAD) is one of the CVDs that is characterized by insufficient delivery of oxygen and blood to the myocardium of heart. CAD occurs due to plaque formation that hinders blood supply in the coronary arteries and lack of oxygen supply which leads imbalance in oxygen demand-supply. It is the major cause of death in the US and worldwide (Shahjehan & Bhutta, 2022). CAD paves the way for a suitable environment for MI i.e., having prior CAD most likely causes MI. Multiple factors are involved that worsen ischemic heart condition ultimately leading to MI (Ojha & Dhamoon, 2021). Thrombus formation in the lumen of the arteries making a barrier in blood passage eventually leads to acute MI which results in heart failure and sudden death (Roth *et al*., 2020).

1.1 Prevalence: Global and National level

The mortality rate of CVDs varies from high income countries to low-income countries. In developed countries CVDs, especially CAD prevalence has been decreasing because of better public health policies that include community intervention to minimize the risk burden of coronary heart disease. Thereby in standardized countries the number of ischemic heart patients dying each year has been reduced because of better health services (Hartley *et al*., 2016). In case of low-income countries, the mortality rate of CVDs has been rising and coronary artery disease is most common reason of death in sub standardized communities (Li *et al*., 2023). Developing co countries mortality due to CVDs account for up to 80% of all the deaths worldwide Addition to

limited health services and public interventions, geographical disruptions contribute to the totality of deaths that occurred due to CVDs in low- and middle-income countries (Mohan *et al*., 2023).

Globally, CAD is the most prevalent disease. In 2020, it has taken 382,820 lives. Approximately 20.1 million people between the age of 20 and above died from CAD. Recently, itwas studied that out of 10 deaths, 2 deaths occur due to CAD, under the age of 65. An estimated 17.8 million deaths occurred in 2017 across the globe due to CVDs (Harikrishnan *et al*., 2018). In 2009, 17.3 million people died according to WHO surveystudy. Highlighting the significant number of deaths that occurred due to CAD (Tsao *et al*., 2022)(Álvarez-Álvarez *et al*., 2017).

MI causes 805,000 deaths in the United States annually, out of which 605,000 die from first episode of MI and 200,000 deaths are those having previous heartattack history (Tsao *et al*., 2022). In 2020, 18.9% out of all the deaths occurred due to MI in Asian population (CDC, 2022).

South Asian populations show much higher prevalence and incidence of MI along with abnormally early age of onset for MI (Sucato *et al*., 2022). In the province Punjab, the incidence of cardiovascular disorders was 17.5% contributing to the total prevalence of CVDs in Pakistan (WHO, 2022).

1.2 Prevalence: Global and National level

MI, also known as “heart attack” is a result of complete or partial blockade of blood flow to myocardium of heart. The specific region of myocardium deprived of blood supply becomes infarct and ischemic. MI or heart attack leads to sudden death if it is not detected. CAD is a common underlying of maximum number of MI. Shortage of blood flow to the myocardium causes deficiency of oxygen, coronary artery disease happens. Deprivation of blood for longer period causes necrosis and apoptosis of cardiomyocytes of myocardium (Ojha & Dhamoon, 2021).

1.3 Oxidative Stress

Oxidative stress is a condition in which production of reactive oxygen species is relatively higher than normal. Therefore, ROS levels become higher than antioxidants and disrupt normal metabolic activities (Rotariu *et al*., 2022). In the case of cardiovascular diseases reactive oxygen species (ROS) are largely produced. ROS causes oxidative stress which leads to damage to DNA, cellular environment, and lipid metabolism.

Some of the events e.g., inflammation, apoptosis, fibrosis etc., trigger oxidative stress which ultimately pave the way for myocardial infarction (Ng *et al*., 2023). Overproduction of ROS leads to the progression as well as development of atherosclerosis. ROS initiates metabolic pathways including apoptosis, inflammation, and lipid metabolism (Batty *et al*., 2022). The antioxidant defense system consisting of enzymatic and nonenzymatic components regulates the ROS levels. In case of oxidative stress, the regulation of antioxidant system gets compromised, leading the increased production of pro-oxidant enzymatic system. Pro-oxidant enzymatic systems promote the development of an atherogenic environment (Donia & Khamis, 2021). As soon as atherosclerosis progresses, the plaque ruptures triggering myocardial infarction. In other words, MI is atherosclerotic disease (Fan & Watanabe, 2022).

1.4 Risk factors

The risk factors for myocardial infarction are broadly classified into two categories: modifiable risk factors and nonmodifiable risk factors. Modifiable risk factors that can be controlled include smoking, dyslipidemia, diabetes, hypertension, obesity, sedentary lifestyle, poor oral hygiene, presence of peripheral vascular disease, elevated levels of homocysteine. Nonmodifiable risk factors that cannot be controlled include age, gender, genetics (Mechanic *et al*., 2017).

1.4.1 Obesity

Obesity is a chronic disease which increases the risk of heart diseases. Fat deposition around abdominal region has been associated with cardiovascular diseases. People with obesity are at greater risk of cardiovascular disorder ending up with MI (Lopez-Jimenez *et al*.,2022).

1.4.2 Hypertension

People having high blood pressure developed atherosclerotic plaque ultimately making the person at great risk of lethal cardiovascular diseases (Rapsomaniki *et al*., 2014). Morbidity and mortality of MI is high in patients with previously known record of underlying hypertension (Pedrinelli *et al*., 2012).

1.4.3 Smoking

Smoking is a major risk for atherosclerotic CVDs including MI. Smoking promotes plaque formation, thickens inner linings of arteries and causes oxidative stress (Parmar *et al.*, 2023). In Young adults, smoking has been linked with increased risk of CAD (SoodSingh and Gadkari, 2023). Tabacco constituents present in cigarette smoke ultimately led to CAD in association with

other risk factors of MI. MI cases are significantly larger in people who smoke as compared to non-smokers (Elkhader *et al*., 2016). As compared to men, women had lower incidence of heart attack, ischemic heart disease and CAD. This incidence is linked with less use of smoking among women. Among female population the rate of MI in smokers has been found to be higher than non-smoker women (GardarsdottirSigurdssonAndersen and Gudmundsdottir, 2022).

1.4.4 Sedentary lifestyle

Lack of physical activity has been associated with developing CVDs. Lifestyle changes reduces the risk of MI differentially in men and women. In both men and women physical activity tends to decrease the risk of MI (Hummel *et al*., 2022).

1.4.5 Diabetes

Diabetes is one of the causes of CAD. Adult male patients with diabetes are 2.5 times at higherrisk of heart diseases compared to those without diabetes. Likewise adult female patients with diabetes are 2.4 times at higher risk of heart diseases (Mons *et al*., 2015). Most diabetic patients are prone to CVDs. The rate of heart diseases is 2.5 times higher in men and 2.4 times higher in women in adults' patients with diabetes compared to those without diabetes (Mozaffarian *et al*., 2015).

1.4.6 Non-modifiable Factors

Risk factors that cannot be changed or modified. These factors are fixed, and they include age, gender, and genetics (National library of medicine, 2022).

1.5 Pathophysiology

MI also known as ischemic heart disease occurs when there is inadequate supply of blood to the portion of heart. The blockade in the blood flow is associated with plaque formation. Atherosclerosis plays main role in plaque formation in the arteries ((US, 2010). The atherosclerotic plaque formation in the arteries cause hindrance in the blood flow. Under this condition thrombus formation occurs and leads to occlusion of the vulnerable plaque, The plaque ruptures ultimately and becomes the reason of ischemic death of cardiomyocytes or MI. Ischemic environment for longer period initiates apoptosis and cell death of layers of heart which in turn malfunctions mitochondria. Signaling pathways involving downstream modulators are activated to counter the inflammatory signals and apoptotic signals (Frangogiannis, 2011). The plaque that ruptures trigger necrotic core formation which is associated with MI. Enhance apoptosis in atherosclerosis causes cellular debris to accumulate and normal homeostasisis compromised (Kumar *et al*., 2023).

1.2 Diagnostic strategies

Diagnostic strategies utilizing miRNAs comprise of miRNA profiling. miRNA profiling includes microarray based, qPCR based, cDNA-based strategies as well as sequencing-based applications (L. Gao & Jiang, 2016). qPCR is widely used for expression analysis of miRNAs (Wei *et al*., 2023).

Deep or next generation sequencing which compares targeted miRNA sequence with sequence of known miRNAs is a well utilized diagnostic application (Satam *et al*., 2023). Microarray approachesinvolve cDNA microarrays to make miRNA profiles (L. Gao & Jiang, 2016). All these tools and methods are current state of art interventions for miRNAs as better diagnostic and prognostic biomolecules.

1.3 Importance of miRNA in disease diagnostics

It has been studied that to reduce the burden of CVDs, including myocardial infarction across the globe, accurate diagnosis is necessary (Joseph *et al*., 2017). Early diagnostic markers for MI with high sensitivity and specificity are the need of time (Naito *et al*., 2022). Traditional biomarkers being used for the diagnosis of cardiovascular disorders include cardiac troponins, creatine kinase-MB (myoglobin binding) etc., (Su *et al*., 2020). These diagnostic and prognostic biomarkers prove to be best in the later stages of MI but fail to showaccurate results in the early time after MI (Su *et al*., 2020). Additionally, prognostic biomarkers for cardiac death include Brain Natriuretic Peptide (BNP) which shows left ventricular dysfunction(Dickstein *et al*., 2008) Imaging approaches such as chest radiography, electrocardiography, computed tomography, magnetic resonance imaging and nuclear imaging (SPECT) are in practice after the episode of MI (Minicucci *et al*., 2011) The limitations associated with these methodologies are their non-specific results, difficulty in the diagnosis in early stages, high cost, age and BMI specificity etc., (Q. Wang *et al*., 2020). miRNAs far better than traditional diagnostics (Cruz *et al*., 2020). The abnormal expression of miRNAs has been found in several different disorders and are being considered as prognostic biomarkers for cardiac diseases as well (L. Zhang *et al*., 2018). Several miRNAs are targeted for their diagnostic value in number of different diseases e.g., cancer, cardiovascular etc., such as circulating miRNAs. miRNAs in the circulating blood have been widely studied and stated as more reliable and sensitive prognostic and diagnostic as compared with conventional diagnostic signatures (Condrat *et al*., 2020; Fichtlscherer *et al*., 2010). Circulating miRNAs in the whole blood, serum and plasma are termed as ideal biomarkers for cardiac associated disorders (Chen *et al*., 2008; Glinge *et al*., 2017). Circulating miRNAs are highly sensitive, disease, cell, and tissue specific, reliable due to their

higher stability from rest of the molecular biomarkers (Glinge *et al*., 2017). Several cardiac specific miRNAs are frequently used for MI including miR1, miR-15a, mi-98 and miR133. (Ouyang & Wei, 2021).

1.4 miRNAs

miRNAs are a class of small noncoding RNAs that mediate gene expression by binding to the 3 UTR of the target mRNA. miRNAs halt the expression of its target gene by translational repression or by inhibiting the formation of translational machinery (Almaghrbi *et al*., 2023). There are two pathways canonical and noncanonical. In both miRNA processing pathways, miRNAs after being synthesized from non-coding DNA sequences form primary or pri-miRNAswhich are transformed into precursor miRNAs or pre-miRNA. Pre-miRNA are than converted intomature miRNAs. Some of the proteins that play important role in biogenesis and mechanism of miRNA mediated gene regulation include Drosha, RISC, Dicer, Argonaut etc. In canonical pathway, pre-miRNAs are cleaved by Dicer enzyme whereas in non-canonical pathway, alternative cleavage of miRNAs is independent of Drosha and Dicer takes place (Jiang & Yan, 2016; Santovito & Weber, 2022). miRNA along with RISC (RNA induced silencing complex) complex bind with the target genes whose expression is to be regulated (O'Brien *et al*., 2018)

1.4.1 miR-15a

miR-15a tends to be upregulated in acute myocardial infarction (K. Fan *et al*., 2021). The levels of miR15a are abnormally high after ischemia/ reperfusion injury which occurs because ofischemic heart disease or MI (Liu *et al*., 2012). The study on diabetes link MI showed upregulation of miR15a in patient's blood (Karim *et al*., 2022). Stroke leading to MI is a common medical condition. Stroke patients experience heart attack in later stages (Schlesinger *et al*., 2023). Stroke patients show disrupt levels of miR15a in the plasma sample, making miR15a a good prognostic biomarker for ischemialead stroke (Yang *et al*., 2017). The prognostic value of miR-15a to act as biomarker for cardiac diseases, has also been validated in a study involving type 2 diabetes leading to coronary artery disease including MI (Mahjoob *et al.*, 2022).

1.5 miR-98-5p

miR-98-5p acts as cardioprotective modulator by reducing the apoptotic burden in the cardiomyocytes. In a study on a mice model, it was found that miR-98 levels were downregulated in the infarct regions of heart (Sun *et al*., 2017). In addition to that, a rat model was used to investigate theexpression of miR98. The expression level of mi-R98 was downregulated.

Mi-R98-5p also plays survival role in the myocardium by lowering, oxidative stress and cell death of cardiomyocytes (Zhai *et al*., 2019). The low level of miR-98 in plasma is the indication of a possible risk of coronary artery disease (Sheikh *et al*., 2020). Absence of miR-98 enhances the atherosclerotic plaque formation; thus miR-98 could prove to be an important diagnostic entity for atherosclerosis as well (Yu *et al*., 2023).

1.6 *Bcl-2*

B-cell lymphoma 2 is an important regulator of cell death in various cellular niches. Bcl-2 acts as antiapoptotic protein by suppressing the proapoptotic players including Bax (Bcl-2 Associated X-protein) and Bak (*Bcl-2* associated X protein) (O'Neill *et al*., 2016). Pro-apoptotic protein carries BH3 binding domain where *Bcl-2* binds either direct or indirect binding (Carrington *et al*., 2017). The survival role of Bcl-2 has been investigated in many studies on cancer where Bcl-2 inhibits apoptosis pathways (Liao *et al*., 2019). During MI, more and more apoptotic players were activated resulting in an enhanced level of apoptosis. It has been reported in MI rat model, Bcl-2 expression was significantly downregulated indicating apoptosis signaling of Bcl-2 to be a promising diagnostic approach in heart disease like MI (J. Cai *et al*., 2022). Bcl-2 is a target of miR-15a and binding of miR-15a with Bcl-2 promotes apoptosis (Ghaffari *et al*., 2021). The abnormal expression of Bcl-2 in cardiomyocytes during MI has been delineated in several studies (C.-K. Gao *et al*., 2016). It has also been stated in reported study that Bcl-2 is downregulated in MI because of significant enhance proapoptotic protein such as Bax (Qiao & Xu, 2016).

1.7 ET-1

Endothelin-1 is a short polypeptide which is involved in the regulation of endothelial function. Et-1 plays an important role in vasoconstriction, atherosclerotic plaque development as well as inflammation in cardiac myocytes (Dąbek *et al*., 2022). The expression of ET-1 in myocardial infarct patients with non-STEMI tends to be abnormally high (Lyu *et al*., 2023). The same high expression of ET-1 is also observed in STEMI patients (Dąbek *et al*., 2022). ET-1 diminishes the hypertension pathway and enhances atherosclerosis by transfer of vascular smooth muscle cells (Lin *et al*., 2015). Inflammation, hypoxic and ischemic environments are major events that activate ET-1. Inflammatory pathways are dysregulated in MI. ET-1 activates IL-6, TNF-alpha and regulates macrophages thus acting as pro-inflammatory modulator. ET-1 enhances oxidative

stress and disrupts lipid metabolism (Aliska *et al*., 2022; Haryono *et al*., 2022; J. Zhang *et al*., 2019). The enhanced expression of ET-1 and its subtype (big ET-1) in the plasma highlights the prognostic value of ET-1 to act as independent factor for MI (Eitel *et al*., 2010; P. Fan *et al*., 2021; Perez *et al*., 2016).

1.8 Bax

Bax (Bcl-2 associated X protein) is one of the pro-apoptotic proteins of Bcl-2 protein family. At the onset of coronary artery blockade which leads towards MI, Bax levels are upregulated due to high apoptosis signaling (Budhram-Mahadeo *et al*., 2014). Moreover, Bax expression levels are significantly enhanced at the time and after myocardial infarction. This over activation of Bax escalates apoptotic signaling in MI (Chi *et al*., 2019). Bax in association with another proapoptotic protein Bak binds at mitochondrial outer membrane initiating apoptosis pathway (Moldoveanu *et al.*, 2023).

1.9 Nfatc3

Nfat is a cardiac hypertrophic marker which plays crucial role in progression of cardiac hypertrophy (Schirmer *et al*., 2018). Nfatc3 is activated during myocardial infarction and hinders the expression of voltage gated potassium channels leading towards cardiac arrythmias (Nieves-Cintrón *et al*., 2016). In addition to this, Nfatc3 regulates cardiac hypertrophy by taking part in mitochondrial dynamics via several signaling pathways (T. Wang *et al*., 2020). In cardiac hypertrophy over expression of Nfatc3 leads to the activation of Nfatc3-calcineurin/calcium which is major hypertrophic stimuli in cardiomyocytes (R. Cai *et al*., 2015).

1.10 Aims and objectives

The purpose of the study is to investigate the role of miRNAs as a diagnostic biomarker for myocardial infarction. Followings are the objectives of the study.

- To check the mRNA expression and protein expression of target genes of miR-15a and miR-98-5p.
- To study the effect of *Bcl-2* apoptotic pathway in myocardial infarction.
- To investigate oxidative and antioxidant profiles in experimental group.

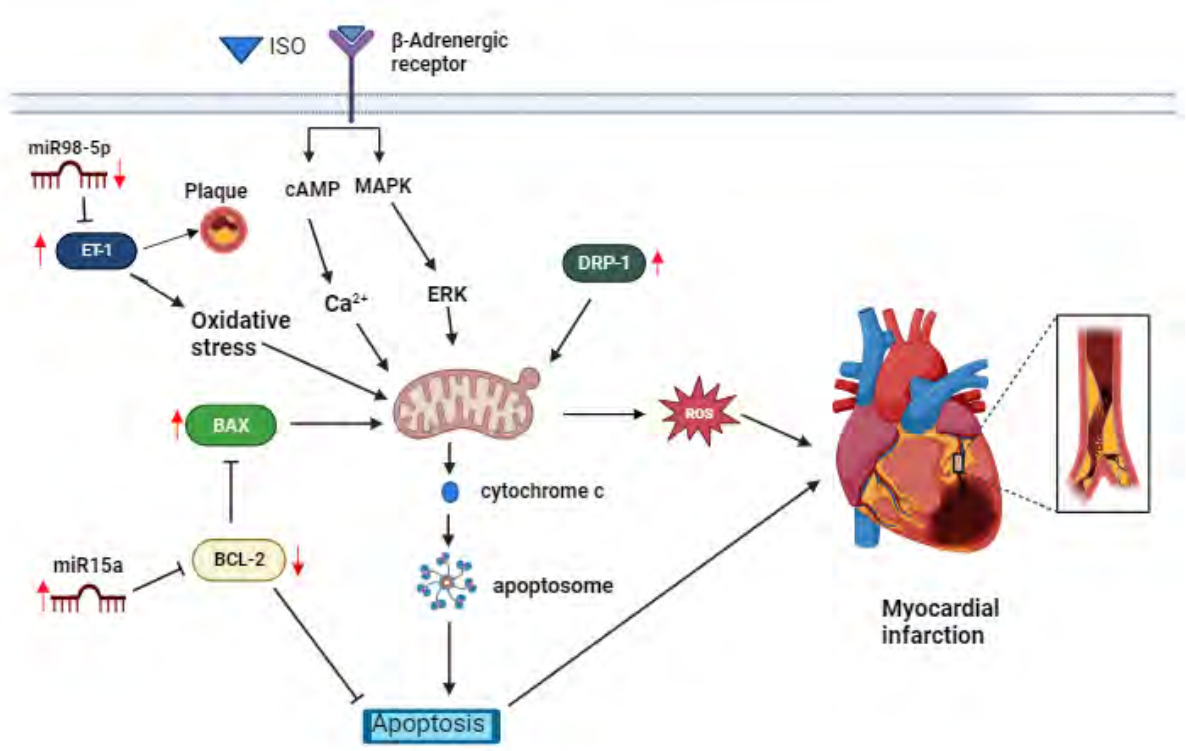

Figure 1.1 Signaling cascade of Isoproterenol induced apoptotic pathway.

2 MATERIALS AND METHODS

2.1 Study Hypothesis

This study was designed to analyze the expression of genes and their downstream signaling pathways involved in apoptosis, therefore for that purpose *Bcl-2* an antiapoptotic gene was chosen. It has anti-apoptotic effects on various physiological and pathological conditions. The present study has focused on MI and aimed to explore the significant role of *Bcl-2* in MI. Bcl-2 may disrupt mitochondrial function and inhibit apoptosis in both heart tissues through ROS formation inhibition and by altering the expression of several proteins such as, Bax and Drp1. Therefore, this study was proposed to check the expression of proapoptotic proteins and antiapoptotic proteins. Moreover, our Aim was to investigate the role of *Bcl-2* in MI as a promising diagnostic target. In the current study miRNA was used as a diagnostic marker for MI.

2.2 Sample Collection of CAD Patients

According to ACC/AHA guidelines (Fihn *et al*, 2014), 122 individuals with angina who presented to AFIC Rawalpindi were recruited for the study. Nine individuals were omitted because they did not meet the inclusion criteria (n = 6) or were unwilling to participate (n = 3). The study included 58 cases of both genders, ranging in age from 25 to 70 years, from a total of 113 individuals. Patients with angina who tested negative for high sensitivity troponin-I (hs-trop-I) and had 50% coronary artery stenosis were diagnosed with CAD according to criteria (Fihn et al, 2014) and were included in the study after giving informed permission or consent. Whole blood samples of CAD patients were collected in EDTA tubes and further expression analysis was done. as well as an animal model using Rats was selected for the study. The altered expression of genes due to apoptosis was determined by qRTPCR and the results were further interpreted by the western blotting. Finally, the results were compiled.

2.3 Ethical Consideration for CAD patient's samples and Animal Models

Whole Blood samples were collected from CAD patients following complete ethical guidelines. We have chosen Sprague Dawley rats for the experiment rats. Rats were kept in the primate facility at Quaid-i-Azam University, Islamabad. A proper recommended diet was given to the rats along with clean water and controlled temperature conditions. Experiments were performed accordance with the Helsinki USA and National Institute of Health (NIH) Islamabad Pakistan. The Ethical Committee of the University provided complete guidelines to perform experimentation.

2.4 Establishment of animal model and the Dosage Regimen

Sprague Dawley rats were selected for the study. Consecutive 14 days of Isoproterenol dosing was given through subcutaneous route. Rats were sacrificed after the completion of dosing period. Organs were collected for homogenate preparation. Rats of the average weight 110-180g were chosen and distributed into two primary groups i.e., disease and control. 5 mg per kg of Isoproterenol was administered subcutaneously to induce myocardial infarction. Isoproterenol group received respective doses subcutaneously and for consecutive 14 days. The normal group was given normal saline for 14 days via subcutaneous route ofadministration.

2.5 Tissue Collection of Animal Model

At the end of the dosing protocol that included optimum weight of rats, dose induction and dissection of rats. Heart was taken, weighed, and saved in -80° for further analysis. Heart was excised into different sized portions for RNA extraction and homogenization preparation. Heart pieces selected for RNA extraction were treated with 200µl TRIzol along with mincing with the help of sharp blades. Heart pieces selected for homogenization were treated with 200µl of extraction buffer. Pieces of heart designated for histological analysis were preserved Eppendorf containing 10% formalin.

2.5.1 Tissue Homogenization

For several biochemical analysis tissue homogenization was done.

2.5.2 Extraction Buffer

Reagents with required concentrations of extraction buffer

Reagents	**Concentration**
HEPES (pH 7.0)	50mM
Phenyl methylsulfonylfluoride (PMSF)	25mg/ml
Sodium Azide	0.02%
Sodium Chloride (NaCl)	150mM
SDS	0.1%
Triton X-100	1ml

Procedure

1mg/10ml PMSF was weighed and dissolved in chilled extraction buffer. At first 100mg heart was

weighed and electric homogenizer was used to homogenize in 500µl extraction buffer along with PMSF. The samples were centrifuged at 13000rpm for 10minutes at -4° C after homogenization. For further analysis supernatant was collected and stored at -20° C for further experimentation.

2.6 Protein Quantification by Bradford Assay

Homogenates containing total protein were used for measuring concentration or quantity of protein by BSA assay. In order to generate standard BSA curve dilutions were made from 5M-10M series. We used Multiskan Go Microplate spectrophotometer for measuring the absorbance at 595nm.

Reagents

Reagents with required concentrations of Bradford assay

Reagents	**Concentration**
BSA serial dilutions	5-10 M
Distilled Water	4 ml
Bradford Reagent	1 ml

Procedure

1 ml of Bradford reagent and 4ml of water was taken to prepare working solution of Bradford reagent i.e1:4 ratio. The Reagents and protein were in 1:40. Then incubation was done for 30 minutes at 37°C. For absorbance, the microtiter plate was placed in Multiskan GO spectrometer (Thermofisher Scientific USA). To plot standard BSA curve the linear equation was used. After obtaining BSA curve, we quantified protein samples.

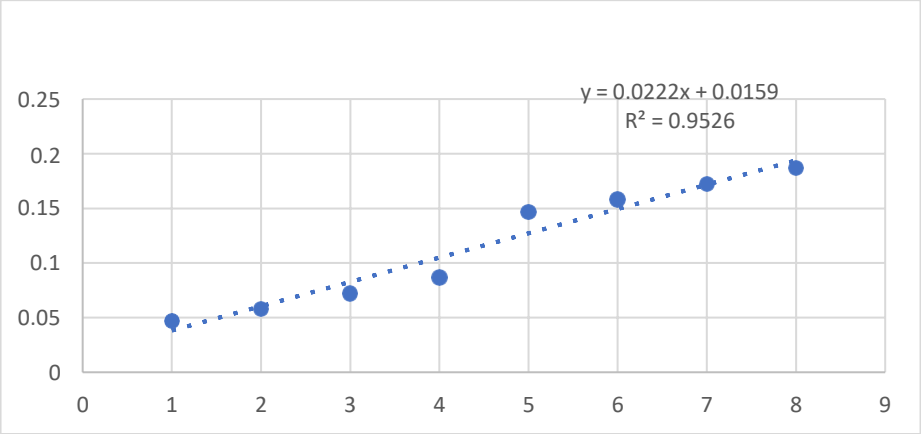

Figure 2.1 Graph Showing Standard Curve for BSA

2.7. Oxidative Profile

For the study of oxidative profile Reactive Oxygen Species (ROS) and Thiobarbituric Acid Reactive Substances (TBARS) level were analyzed.

2.7.1. Estimation of ROS by Reactive Oxygen Species (ROS) Assay

(Hayashi et al., 2007) Protocol was followed for detection of ROS level in tissue homogenates and serum samples.

Reagents with concentrations of ROS assay

Reagents	Concentration / Volume
Reagent 1: N, N-Diethyl para-phenyl diamine (DEPPD)	1 mg/ ml
Reagent 2: Ferrous sulfate (FeSO4)	0.5%
Sodium Acetate Buffer (pH 4.8)	0.1 M PH 4.8
Sample	6.6 µl

Procedure

Reagent1 was added in Reagent 2 for the preparation of reagent mixture in a ratio of 1: 24 and placed in dark for 2 minutes. 133.3 µl of reaction buffer, 6.6 µl of sample and 186 µl of reagent mix were added in each well of microtiter plate. At 505 nm the absorbance was measured by multiskan GO (Thermo-Fischer scientific, USA) spectrophotometer. At 505 nm three readings were recorded at interval of 15 seconds. A standard curve of H_2O_2 was generated.

2.7.2. Estimation of Thiobarbituric acid Reactive substances (TBARS) level

TBARS activity in homogenates and serum was estimated according to the protocol given in (Tsai et al., 2014).

Reagents

Reagents with the concentrations used in TBARs assay.

Reagents	Concentration / volume
Tris -HCL	150 mM
Ascorbic acid	1.5 mM
Ferrous sulphate	1 mM
Trichloroacetic acid	10%
Thiobarbituric acid	0.375%
Sample	20 µl

Procedure

20 µl of Tris HCL, 20 µl of sample, 20 µl of ascorbic acid and 20 µl of $FeSO_4$ along with 120 µl distilled water was added in an Eppendorf and incubated at 37 C for 15 min. From that point onwards 200 µl of TCA and TBA was added. Incubation of Eppendorf was done at 100 C^o for 15 min. Whole material was shifted for the centrifugation at 3000 rpm for 10 minutes. Supernatant of 200 µl was then picked and added in each well of microtiter plate. With the help of multiskan GO (Thermo-Fischer scientific, USA), three consecutive absorbances were taken at 532 nm. Lipid per oxidation level was calculated by the formula mentioned below:

TBARS (nM/mg of protein) = Optical density x Total volume x 1.56 x 105 x mg of protein / ml.

2.8. Analysis of Antioxidative status

2.8.1. Super Oxide Dismutase (SOD) Assay

In serum and tissue homogenates SOD activity was measured as described in (Ali, Waheed, et al., 2015).

Reagent recipe of SOD assay

Reagents	Concentration
Phosphate buffer saline	50 mM, pH 7.8
L-Methionine	9.9 mM

NBT	57 µM
Triton	0.025 %
Riboflavin	0.9 µM
Sample	5 µl

Procedure

In order to prepare reagent mixture 1.5 ml L-Methionine, 1 ml NBT.2HCL and 750 µl Triton x-100 were all added and by adding phosphate buffer saline volume was raised up to 30 ml. In each well of plate 250 µl of this mixture was added. After that 5 µl of serum sample was added. Fluorescent light was given to the whole reaction microtiter plate by using lamp at 37 ºC for 7 minutes. Afterwards 2 µl of chilled riboflavin was added. Plate was kept under incubation for the initiation of reaction at 40 ºC for 8 minutes. Later the Absorbance was measured thrice for each sample by multiskan GO (Thermo-Fischer scientific, USA) spectrophotometer at 560 nm with the time interval of 1 minute. The formula mentioned below was used for the calculation of percentage inhibition of NBT.

(Abs. $_{Blank}$ - Abs. $_{sample)}$ / (Abs.$_{Blank}$) X 100

2.8.2 Catalase Activity (CAT) Assay

The protocol described in (Ali, Shaheen, et al., 2015) was utilized to measure the activity of CAT. For the estimation of catalase activity in serum samples following reagents were required.

Reagents given with required concentration to be used in CAT assay

Reagents	**Concentration / Volume**
Potassium phosphate buffer	50 mM, pH 7
Distilled hydrogen per oxide	5.9 mM
Samples	11.1 µl

Procedure

In each well of microtiter plate 222 µl of buffer, 111 µl of H_2O_2 and 11.1 µl of serum sample were added. All reagents except sample were taken as a blank except sample. Absorbance for each sample was measured by multiskan GO (Thermo-Fischer scientific, USA) spectrophotometer at 240 nm. With a time, interval of 30 seconds three readings was calculated.

2.8.3. Peroxidase (POD) Assay

For the measurement of POD activity of enzyme following reagents were required.

Reagents

POD assay recipe of regents with optimum concentrations

Reagents	**Concentration / Volume**
Phosphate buffer	50 mM, pH 5.0
Hydrogen per oxide	40 mM
Guaiacol	20 mM
Samples	6.7 µl

Procedure

In each well of microtiter plate 166.6 µl of phosphate buffer, 6.7 µl (50 mM) of Guaiacol and 6.7 µl of sample was added respectively. Stirring of the mixture was done forcefully. H_2O_2 was added in the mixture at the end. Multiskan GO (Thermo-Fischer scientific, USA) spectrophotometer was used to measure absorbance at 420 nm. With a time interval of 1 minute three readings were calculated.

2.8.4. Ascorbate Peroxidase Assay

Reagents

Reagents of APX assay with required concentrations

Reagents	Concentration / Volume
Potassium phosphate buffer	50 mM, pH 7
EDTA	5 mM
Ascorbate	1 Mm
Hydrogen peroxide	1 mM
Sample	10 µl

Procedure

In each well of microtiter plate, 60 µl of Potassium phosphate buffer, 10 µl of EDTA, 10 µl Ascorbate, 10 µl H_2O_2 and 10 µl of sample were added. multiskan GO (Thermo-Fischer Scientific, USA) spectrophotometer was used to measure the level of ascorbate in serum samples by measuring the absorbance at 290 nm and taking three readings. With the help of formula mentioned below the level of ascorbate peroxidase was estimated:

Activity of Ascorbate = Absorbance X Extinction Co-efficient of Ascorbate.

2.8.5. Reduced Glutathione Assay

Reagents

Reagents recipe with the amount of concentration of reagents used in GSH assay.

Reagents	Concentration
3,3-dithi-bis (6-nitrobenzoic acid) DTNB	0.4%
Sodium Phosphate buffer	11.356 g, 0.4 M
Serum sample	5 µl

Procedure

In each well of microtiter plate 5 µl of sample, 50 µl of sodium phosphate and 25 µl of DTNB were added. yellow color was appeared. Absorbance was measured by multiskan GO (Thermo-Fischer scientific, USA) spectrophotometer at 412 nm.

2.9. Lipid profile

Triglyceride and cholesterol assays were performed to get results for lipid profile

2.9.1. Cholesterol assay

According to the protocol given in AMP (AMEDA Labordiagnostik GmbH; Austria) diagnostic kit cholesterol assay was performed.

Principle

Enzymes *i.e.* peroxidase, cholesterol oxidase and cholesterol esterase contain Hydrogen peroxide that would condensed the reaction mixture containing 4-aminoantipyrine and phenol as a result quinonimine dye was formed. The amount of cholesterol in the sample is proportional to the concentration of quinonimine dye.

Given are the volumetric amounts of reagents of cholesterol assay.

Reagents	**Volume**
Cholesterol reagent	200 µl
Sample	2 µl
Standard	2 µl

Procedure

200 µl of reagent and 2 µl sample was added in each well of the microtiter plate. 2 µl of standard in 200 µl of reagent was also added in a separate well. Incubate for 5 minutes at 37 ºC. Absorbance of sample and standard was taken at 500 ºC from multiskan GO (Thermo-Fischer scientific, USA) spectrophotometer three times. Readings were calculated from the formula given in the kit.

Total cholesterol (mg/dL) = Sample $_{abs}$ / Standard $_{abs}$ X Concentration of standard

2.9.2. Triglycerides

Triglycerides assay was performed according to the protocol given in AMP (AMEDA Labordiagnostik GmbH; Austria) kit. following reagents were used:

The reagent recipe of triglyceride assay

Reagents	**Volume**
Triglyceride reagent	200 µl
Sample	2 µl
Standard	2 µl

Principle

Triglycerides are converted to fatty acid and glycerol after metabolism. Glycerol is phosphorylated by glycerol kinase in the presence of ATP into glycerol-3-phosphate (G-3-P). Glycerol-3-phosphate (G-3-P) is oxidized into dihydroxyacetone phosphate and hydrogen peroxide by glycerol-phosphate oxidase enzyme.
Followed by the formation of hydrogen peroxide the peroxidase enzyme catalyzes the reaction between 4-aminoantipyrine and phenol with hydrogen peroxide. A red color is produced as a result of this reaction. The concentration of triglycerides in the sample is directly proportional to the concentration of triglycerides in the sample.

Procedure

In each well of the microtiter plate, 200 µl of reagent and 2 µl sample. In a separate well, 2 µl of standard in 200 µl of reagent was also added. Incubate at 37 ºC for 5 minutes. At 500nm absorbance of sample and standard was taken repeatedly three times from multiskan GO (Thermo-Fischer scientific, USA) spectrophotometer. With the help of formula given in the kit readings were calculated.

Total triglyceride (mg/dL) = Sample $_{abs}$ / Standard $_{abs}$ X concentration

2.10. Liver function tests

Liver functions were analyzed by performing ALT and AST assays.

2.10.1. Alanine Aminotransferase (ALT) Assay

ALT enzymes levels in serum were checked by the following protocol given in AMP (AMEDA Labordiagnostik GmbH; Austria) diagnostic kit.

Following reagents were used:

Reagents with required concentrations for ALT assay

Reagents	**Concentrations / Volume**
Reagent 1 (Tris-buffer, L-Alanine, Lactate dehydrogenase)	150 mM PH 7.3, 750 mM > 1.350 U/L
Reagent 2 (NADH, 2-Oxoglutarate, Biocides)	1.3 mM, 75 mM
Serum sample	10 µl

Procedure

For preparing rection mixture Reagent 1 and Reagent 2 were mixed in 4:1. In each well 200 µl of reaction mixture was added along with 10 µl of sample. Incubation for 1 min was given at room temperature. Initial absorbance at 340 nm was recorded by multiskan GO (Thermo Fischer scientific, USA) spectrophotometer. For taking 3 readings same incubation steps were performed in a repetition. With the help of formula given in the kit, the level of ALT in serum was calculated.

ΔA/ min X 3333 = ALT activity (unit/ liter).

2.10.2. Aspartate Aminotransferase AST

To check Aspartate Aminotransferase enzymes levels in serum, AMP diagnostic kit protocol was followed.

Principle

Aspartate amino transferase enzyme functions by transferring amino group. Malate dehydrogenase (MDH) reduce oxaloacetate. NADH is reduced to NAD + which decreases the absorption. Absorption is proportional to the activity of AST. Following were the reagents used

Optimal concentration of reagents for AST assay

Reagents	**Concentrations / Volume**
Reagent 1 (Tris-buffer, L-aspartate, NADPH, MDH, LDH)	121 mM PH 7.8, 362 mM > 460 U/L, >600 U/L
Reagent 2 (NADH, 2-Oxoglutarate, Biocides)	1.3 mM, 75 mM
Sample	10 µl

Procedure

According to the number of samples R1 and R2 were mixed in 4:1 .200 µl of reaction mixture in each well were added along with 10 µl of sample. Incubation for 1 min was given at room temperature. Initial absorbance at 340 nm was recorded by multiskan GO (Thermo Fischer scientific, USA) spectrophotometer. For taking 3 readings same incubation steps were performed in a repetition. With the help of formula given in the kit, the level of AST in serum was calculated.

ΔA/ min X 3333 = AST activity (unit/ liter).

2.11. Western Blotting

We performed western blot analysis to identify the expression of protein in samples. Ma (2006) protocol was followed for western blotting. The western blotting apparatus of Bio-Rad us was used in this procedure. To identify the expression of proteins in different experimental groups Western

blot analysis was carried out. It was done according to Ma (2006) protocol by using the western blotting apparatus of Bio-Rad USA.

Steps

Steps for western blotting were as follows:

- Gel preparation
- Transfer of protein on nitrocellulose membrane
- Blocking
- Antibody (primary and secondary) treatment
- Detection of chromogenic substrate

2.11.1. Gel Preparation and Electrophoresis Gel Preparation:

Following reagents were used for gel preparation

Reagents	Separating gel (12%)	Stacking gel (4%)
Distilled Water	1672µl	3020 µl
Tris- HCl	1250 µl (1.5M,PH 8.8)	1250 µl (0.5M,PH 6.8)
SDS (10%)	50 µl	50 µl
Acr-Bis (30%)	2000 µl	650 µl
AP (10%)	25 µl	25 µl
TEMED	3 µl	5 µl

Procedure:

We set the Gel casting apparatus. At first, we prepared 12%Gel casting apparatus was set. First 12% separating gel and carefully poured it along with isopropanol on the top of gel ro remove air bubbles. We let the separating gel to solidify. After solidification of gel, isopropanol was

discarded. The gel was then washed with distilled water thrice and dried with the help of filter paper. We prepared 4% stacking gel and poured it onto the dried polymerized separating gel. Then we inserted the comb for well formation. After placing the comb, we left stacking gel for solidification. Just after the polymerization of stacking gel, the casting frame was removed from gel cassette and was camped on the clamping frame. The samples were than prepared for loading into the gel.

2.11.2. Sample Preparation

Reagents

Following reagents were needed for sample preparation.

Reagents for 2X SDS-Gel Loading Buffer (100 ml)

Following Reagents are required for the making Loading buffer

Reagents	**Concentration**
Glycerol	0.2%
Dithiothreitol	200mM
Tris-HCl	62.5 mM, pH 6.8
Bromophenol blue	0.01%
Sodium dodecyl sulfate	2%

Procedure

To make up final volume of 19 µl extraction buffer, SDS loading dye and samples were mixed. Incubation of mixture was done for 10 minutes at 95˚C in a water bath. Afterwards centrifugation was done for 1 min at 2000rpm.

2.11.3. Sample Loading and Gel Running

Recipe for 5X SDS Running Buffer (1000 ml)

Reagents	**Concentration**
Tris	125mM

SDS	0.50%
Glycine	1.25M

In order to make 1000ml 1X SDS running Buffer, 800ml distilled water was added in 2ml 5X SDS Running Buffer.

Procedure

The samples were loaded into wells after filling the gel tank with 1X SDS gel running buffer, two gel plates were clamped in a clamping equipment, the comb was removed. Ladder (a known protein marker) was loaded in the first. Initially gel was run at 90V.When the loading dye reached the polymerized separating gel then 120V voltage was applied, again loading dye was observed till it reached end of plates and fully resolved. Gel was first stained with Coomassie R-250 to confirm the expression of proteins and procedure along with reagents is as follows:

2.11.4. Gel Staining

Reagents

Fixing Solution

Given are the volumetric amounts of reagents of fixing solutions.

Reagents	**Concentration**
Methanol	50%
Glacial acetic acid	10%
Distilled water	Remaining volume

Staining Solution

The volumetric amounts of reagents of staining solution

Reagents	**Concentration**
Coomassie R-250	0.1%
Methanol	50%

Glacial acetic acid	10%
Distilled water	Remaining volume

Destaining Solution

Concentration of reagents required for Destaining solution

Reagents	**Concentration**
Methanol	40%
Glacial acetic acid	10%
Distilled water	Remaining volume

Storage Solution

Concentration of glacial acetic required for storage solution

5% glacial acetic acid

Procedure

Fixing solution was taken and gel was placed in it after it was carefully removed. After that it was left for overnight incubation. Afterwards fixing solution was discarded, and gel was stained in staining solution for 20 minutes. After staining for 20 minutes, the staining solution was discarded. The destaining solution was used to destain the gel, destaining solution was in destaining solution, destaining solution was replaced several times until background of gel was fully destained, subsequently bands were observed. Gel staining was not performed on gels that were transferred to nitrocellulose membrane.

2.11.5. Transfer of Proteins on Nitrocellulose Membrane

Reagents

Following reagents were required for blotting.

Transfer Buffer

Reagent recipe of Transfer buffer

Reagents	**Concentration**
Glycine	192 mM, 14.04 g

Tris	25 mM
Methanol	20 %, 200 ml
Distilled Water	Remaining volume

Phosphate Buffer Saline (pH 7.4)

Reagents with required concentration are given

Reagents	**Concentration**
Potassium chloride (KCl)	2.7mM
Sodium Chloride (NaCl)	150mM
Potassium dihydrogen phosphate (KH_2PO_4)	1.8 mM
Di sodium hydrogen phosphate (Na_2HPO_4)	10.1 mM
Distilled Water	Remaining volume

Ponceau Stain

Concentration of reagents required for Ponceau Staining

Reagents	**Concentration**
Ponceau stain	0.5 g
Glacial acetic acid	5 ml
Distilled water	Remaining volume

Phosphate Buffer Saline (1 L, pH 7.4)

100 µl Tween-20 in 100 ml of PBS

TBST

Given are the reagents of TBST with standard contractions.

Reagents	**Concentration**
Tris base (1M), pH 8	1M 50ml
Sodium chloride (NaCl)	3M 100ml

Tween-20	2ml
Distilled water	Remaining volume

Procedure

At first, twelve filter papers of similar size and nitrocellulose membrane (NC) were soaked in transfer buffer and placed on blotting equipment in such a manner that the nitrocellulose membrane was sandwiched between the filter papers and gel was placed above the nitrocellulose membrane for 30 minutes. Ponceau stain was applied to the membrane to verify protein transfer. Membrane was then washed with TBST.

2.11.6. Blocking

Composition of Blocking Solution

The blocking solution composed of 5% solution of non-fat dry milk prepared in phosphate buffer saline was used.

Procedure

Membrane was soaked in blocking solution for 45 minutes to block nonspecific binding and then washed with TBST three times.

2.11.7 Antibody Treatment

Primary Antibodies

Following proteins with primary antibodies for antibody treatment

Proteins	Primary Antibodies
GAPDH	Mouse monoclonal; Solis BIO
BAX	Mouse monoclonal; Santa Cruz
NFATC3	Mouse monoclonal; Santa Cruz
DRP-1	Mouse monoclonal; Santa Cruz
ET-1	Mouse monoclonal; Santa Cruz

Secondary antibodies

Following proteins with secondary antibody for antibody treatment

Target Proteins	Secondary antibodies
GAPDH	Goat Antimouse (IGg) Abcam
BAX	Goat Antimouse (IGg) Abcam
NFATC3	Goat Antimouse (IGg) Abcam
Drp1	Goat Antimouse (IGg) Abcam
ET-1	Goat Antimouse (IGg) Abcam
Tubulin- α	Goat Antimouse (IGg) Abcam

Dilution of Antibody Solution

0.01% Bovine serum albumin in TBST

Primary antibodies were diluted at ratio of 1:5000 and secondary at 1:2000.

Final Washing Buffer

Reagent recipe for washing buffer

Reagents	Concentration
Tris HCl	6.05g in 50ml D. H20
NaCl	17.52g in 100ml D. H20
Distilled water	Remaining volume

Procedure

The primary antibody was treated with the membrane and left at -4 ˚C for overnight incubation followed by three times washing with TBST. After that, the membrane was treated with secondary antibody at room temperature for 2 hours while being shaken. Secondary antibody was discarded after an hour and washed NC twice for 5 minutes with final washing buffer.

2.11.8. Detection of Chromogenic substrate

BCIP (5-bromo-4-chloro-3'-indolylphosphate) \ NBT (Nitro blue Tetrazolium)

Procedure

For 30 minutes 1000µl substrate solution was applied on NC.

After half hour the observation of the bands was done and photographed. For densitometric analysis the Fiji/ImageJ software was used for densitometric analysis.

2.12. Quantitative Real Time PCR Analysis

To identify the expression of targets genes in different experimental group's Quantitative real time PCR analysis was performed.

Basic steps:

- RNA extraction from Heart Tissues and Blood samples
- cDNA synthesis
- Quantitative real time PCR

2.12.1. RNA/miRNA Extraction from Heart Tissues and Blood samples

Following reagents were required for RNA extraction from all samples.

Reagents	**Concentration**
Chloroform	50 µl
TRIzol	100 µl
Isopropanol	150 µl
Glycogen	1 µl
Ethanol	70%
DEPC treated water	25 µl

Procedure

RNA extraction was performed to obtain high quality RNA from blood samples of patient, control, and blood from rat's heart. Chemicals required for RNA extraction include chloroform dissolved in phenol, glycogen, TRIzol, isopropanol, 70% ethanol, distilled water, ice box, syringes 26G (3 ml), pipettes, tips, gloves, centrifuge at 4^{o} C. Samples collected from the patients transferred to

EDTA tube immediately inverted and then transferred in 2 ml Eppendorf. The samples were put into the centrifuge at speed at 13500 rpm for 15 mints. After centrifugation, we discarded supernatant and added 750 µl TRIzol to the pellet containing the blood cells. Then vortex was used to mix the sample with TRIzol. After that, we used 3 ml syringes to mince the cells. Syringing was done for 15 minutes. When we had finished syringing, we added 50 µl chloroform in it. Then we did centrifugation at 13500 rpm for 15 minutes. After centrifugation, we separated aqueous layer from the lower layer containing cellular debris. We transferred the aqueous layer into another Eppendorf. We added 150µl isopropanol and 1µl glycogen, we incubated the samples for another 5 minutes in refrigerator at -4° C(ice). Centrifugation was performed after incubation at 13500 rpm for 15 minutes. At the end of centrifugation, we discarded the supernatant and added 500 µl of 70% ethanol in the Eppendorf. We vortexed the Eppendorf and set them in the centrifugation at 13500 rpm for 15 minutes. Ethanol was discarded after centrifugation. We then air dried the pellets and added 10 µl DEPC and vortexed for few seconds after air dry. We performed nanodrop using DEPC as blank. In order to find concentration of RNA in the samples, Nanodrop (UV/VIS NanoDrop-1000™ (Nanodrop, V3.7, Thermo Fisher Scientific) was utilized using DEPC as blank. 2µl of extraction RNA samples was used for Nanodrop. After quantification of RNA, samples were stored at -80 ° C.

2.12.2. cDNA Synthesis

cDNA synthesis was done using kit method *i.e*. according to instruction provided by "Revert Aid First Strand cDNA Synthesis Kit" (Thermo Fisher).

Reagents

Reaction mixture recipe for cDNA synthesis

Reagents	**Concentration**
Random hexamer primer	1 µl
5X Reaction buffer	4µl
dNTP mix 10mM	2µl
RevertAid M-MuLV RT	1µl
Ribolock RNase Inhibitor	1µl

Procedure

According to kit instruction, nuclease free water, random hexamer primer and sample were mixed according to kit instruction. Incubation of this mixture was done for 5mins at 65˚C. After that remaining reagents of kit were added *i.e*., 4 µl 5X Reaction buffer, 2 µl 10mM dNTP mix, 1µl Ribolock RNase Inhibitor and 1 µl RevertAid M-MuLV RT. The PCR tubes were vortexed and placed in PCR machine for 60 minutes at 42˚C . The cDNA was stored at -20 ºC.

2.12.3. Polymerase Chain Reaction (PCR)

In this study we targeted several genes and performed gradient PCR for optimizing annealing temperature of selected genes. PCR was done according to the instruction of the Thermo-scientific kit. 25 µl reaction mixture was prepared for each sample. Following are the reagents that are used in PCR.

Reagents with required concentration for PCR.

Reagents	**Concentration**
PCR water or nuclease free water	15.6µl
Buffer	2.5 µl
MgCl2	2 µl
Forward primer	1 µl
Reverse primer	1 µl
dNTPs	1 µl
Taq polymerase	0.4 µl
Sample	1.5 µl

Gradient PCR was performed at these conditions

- Hold at 95 º C for 10 minutes
- Denaturation at 95 º C for 10 seconds
- Annealing for 15 seconds

- Extension at 72 ° C
- Total 35 cycles

PCR products were then run on 2% agarose gel and bands were observed by gel doc apparatus.

2.12.4. Quantitative Real Time PCR

Real Time PCR was performed of the stored samples at following conditions.

Reagents

Table showing the reagents of real time PCR recipe of cocktail.

Reagents	**Concentration**
cDNA	2 µl
Gene specific Forward primer	0.37 µl
Gene specific Reverse primer	0.37 µl
Eva green	5 µl
Nuclease free water	2.26 µl

Procedure

2µl cDNA (each sample) was first directly poured in separate PCR vials. Reaction mixture was prepared using nuclease free water (2.26µl) then gene specific forward (0.37 µl) and reverse primers (0.37 µl) were added. 5 µl EVA green was added in this reaction mixture in the end and vortexed for few seconds.2µl cDNA along with 8µl reaction mixture were added in RT tubes and placed RT machine. Desired gene expression of genes was observed in RT-PCR (MyGoPro).

2.13. Histopathology

After dissection of heart, tissues were placed in fixative (formaldehyde 30%) for microscopic analysis. Hematoxylin and Eosin staining was done alone with Masson trichome staining. Microscopic images of the stained slides were observed and analyzed under light microscope.

2.13.1. Microscopic Analysis

These slices were observed under light microscope (DIALUX 20 EB) at 40 X magnification. All the slides were observed and photographed.

2.14. Statistical Analysis

Statistical study was done by means of one-way ANOVA (Analysis of Variance) proceeded by Tukey's Test. The statistics was significant at p-value ≤ 0.01 or ≤ 0.05 which was calculated by use of IBM SPSS (Statistical Program for Social Sciences) USA statistics 21. The graphs were made by using the GraphPad Prism software.

3 RESULTS

3.1. Demographic Data

3.1.1. Gender-wise Distribution

The CAD patients were divided into two groups based on gender as shown in Figure 3.1. The first group comprised of male patients (72.72%). The second group comprised of CAD female patients (27%).

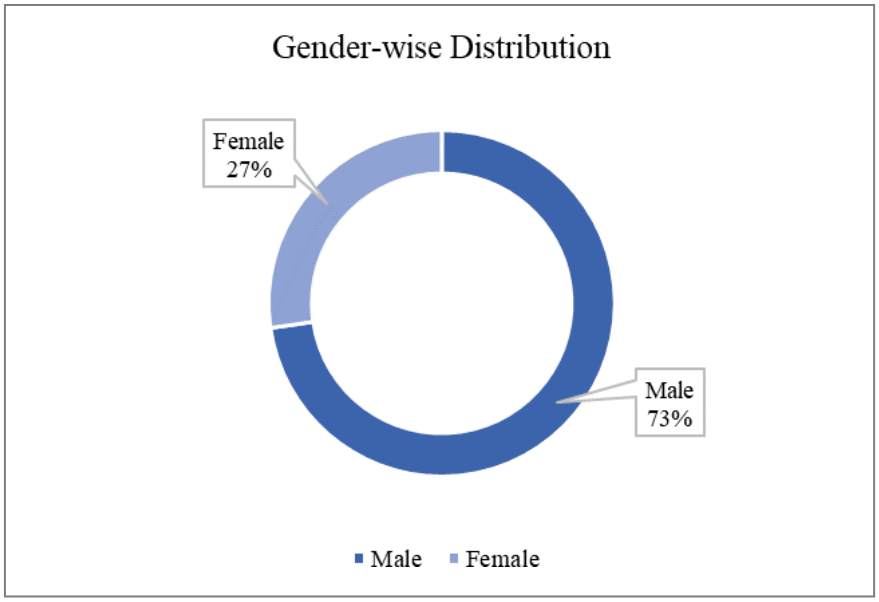

Figure 3.1 Graphical Representation of Gender-wise Distribution of CAD Patients

3.1.2. Age-wise Distribution

The CAD patients were distributed into four groups based on age as shown in Figure 3.2. The first group comprised of CAD patients in the under 20 age group (9%). The second group comprised of CAD patients between 21-40 age group (18%). The third group comprised of CAD patients between 41-60 age group with (27%). The fourth group comprised of CAD patients in the above 60 age group with (45%).

3.1.3. Other Diseases in CAD Patients

It was recorded that no patient suffered from asthma or lung disease. All the patients of myocardial infarction were not diagnosed with liver disease. About 27.27% of CAD patients were suffering from diabetes. It was also recorded that 45.45% of CAD patients were

suffering from hypertension. 45.45% of CAD patients showed high blood pressure as shown in Figure 3.3.

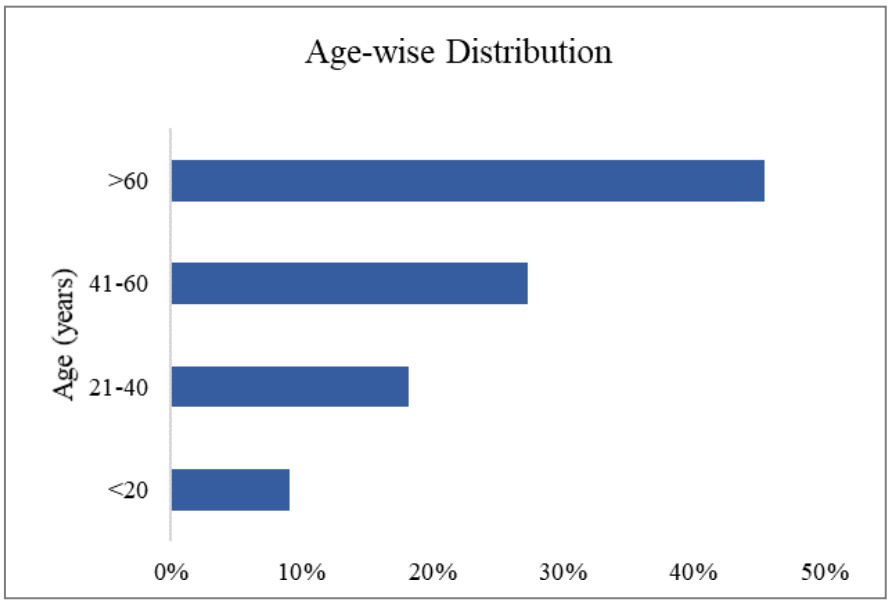

Figure 3.2 Graphical Representation of Age-wise Distribution of CAD Patients

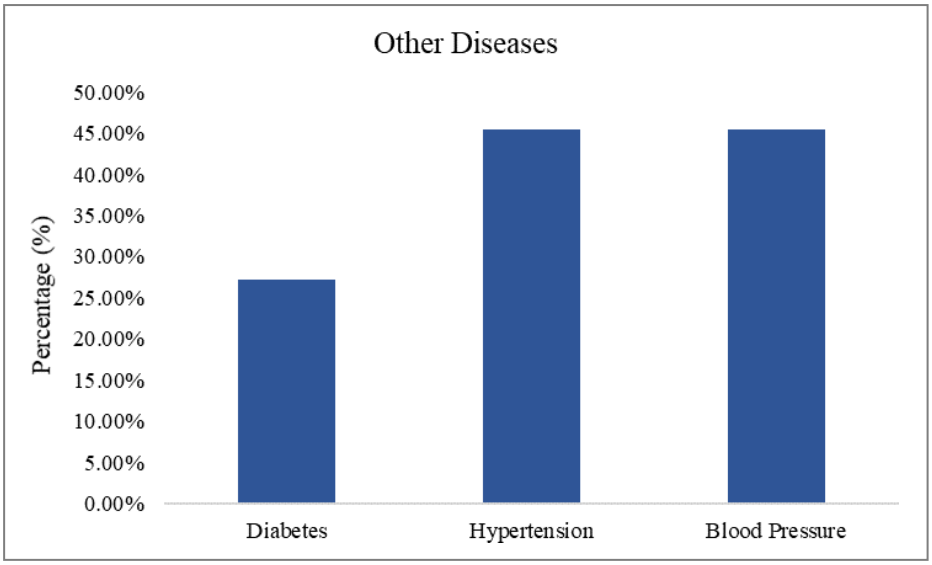

Figure 3.3 Graphical Representation of other diseases in CAD patients

3.1.4. Smoking status of CAD Patients

27.27% of CAD patients were smokers as shown in Figure 3.4 while others werenon-smokers.

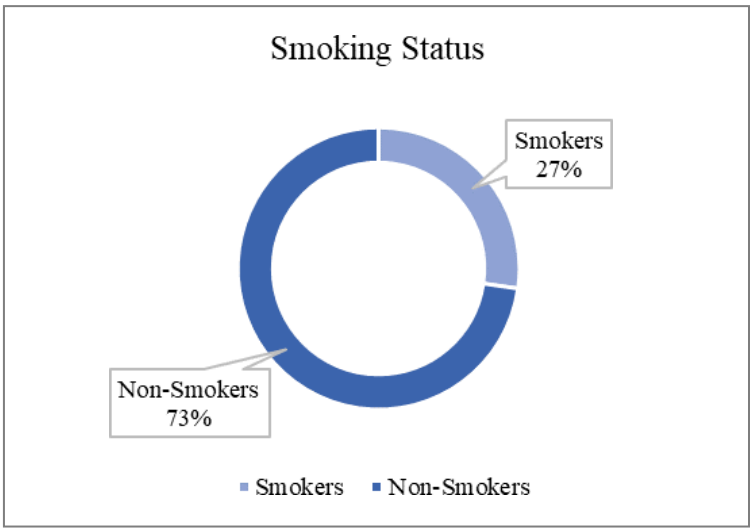

Figure 3.4 Graphical Representation of Smoking Status of CAD Patients

3.1.5. Time since diagnosis of CAD in Patients

27.27% were diagnosed between 3-15 days ago, 18.18% were diagnosed between 2-6 months ago, 9.09% were diagnosed 8 months ago and other patients (45.45%) were diagnosed 2-6 years ago as shown in figure 3.5.

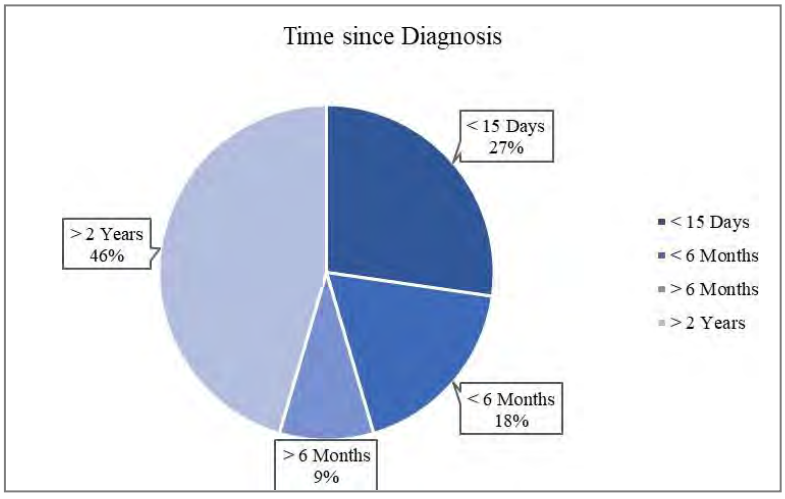

Figure 3.5 Graphical Representation of Time since Diagnosis

3.2. Expression of *Bcl-2* in CAD patient's whole blood

Bcl-2 is an antiapoptotic gene which plays a survival role in normal physiological condition in cardiomyocytes. In myocardial infarction, *Bcl-2* expression was reported to be downregulated. The expression of *Bcl-2* was investigated by qRT-PCR. GAPDH was used as an endogenous control. *Bcl-2* was significantly downregulated in myocardial infarction patient's blood. For statistical analysis, T test was performed by using GraphPad prism version 10.0.0. The graph was plotted in accordance with Mean ± SEM with significance (****) at $p<0.0001$ as shown in Figure 3.6.

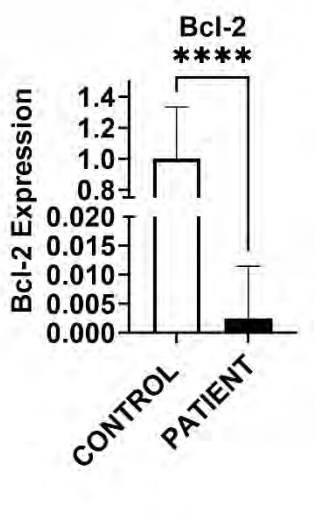

Figure 3.6 Graphical representation of Bcl-2 expression in myocardial infarction patients

3.3. Expression of ET-1 in CAD patient's whole blood

Endothelin-1 is a short polypeptide which is involved in the regulation of endothelial function, vasoconstriction, atherosclerotic plaque development and inflammation in cardiac-myocytes. The expression of ET-1 was investigated by qRT-PCR. GAPDH was used as an endogenous control. Relative fold activity of ET-1 was measured by using Microsoft excel. ET-1 was significantly upregulated in myocardial infarction patient's blood. For statistical analysis, T test was performed by using GraphPad prism version 10.0.0. The graph was plotted in accordance with Mean ± SEM with significance (*) at $p<0.0238$ as shown in Figure 3.7.

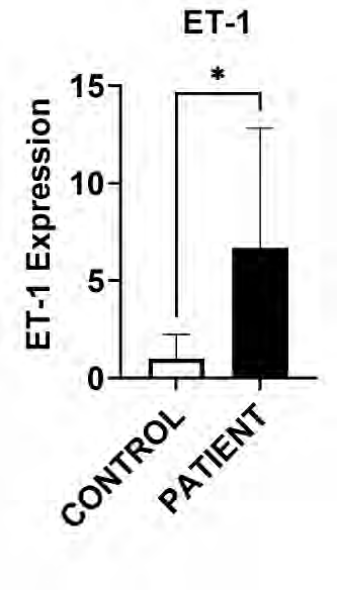

Figure 3.7 Graphical representation of ET-1 expression in myocardial infarction patient's whole blood.

3.4. Expression of NFATc3 in CAD patient's whole blood

Nfatc3 is a cardiac hypertrophic marker which plays crucial role in progression of cardiac hypertrophy. The expression of NFATc3 was investigated by qRT-PCR. GAPDH was used as an endogenous control. NFATc3 was significantly downregulated in CAD patient's blood. For statistical analysis, T test was performed by using GraphPad prism version 10.0.0. Thegraph was plotted in accordance with Mean ± SEM with significance (***) at $p<0.0001$ as shownin Figure 3.8.

3.5. Expression of miR-15a in CAD patient's whole blood

miR-15a is reported to be involved in cardiovascular diseases including acute MI, ischemia/ reperfusion injury, diabetes link myocardial infarction and stroke leading to MI. The expression of miR-15a was investigated by qRT-PCR. U6 was used asan endogenous control. miR-15a was significantly upregulated in CAD patient's blood. For statistical analysis, the T test was performed by using GraphPad prism version 10.0.0. The graph was plotted in accordance with Mean ± SEM with significance (***) at $p<0.0002$ as shownin Figure 3.9

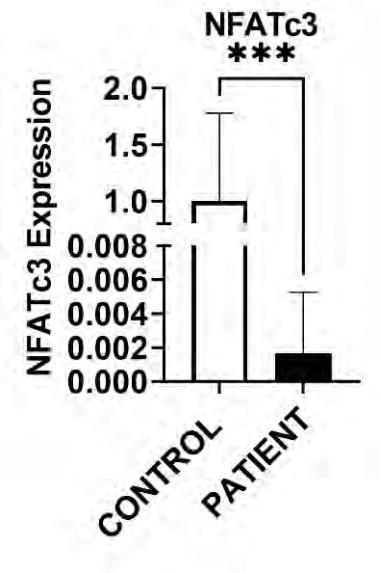

Figure 3.8 Expression analysis of NFAT3 in CAD patient's whole blood.

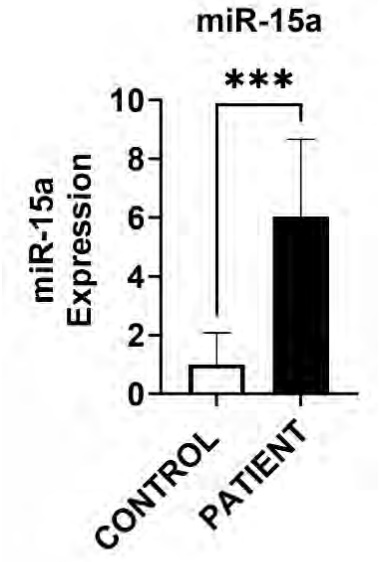

Figure 3.9 Expression analysis of miR-15a in CAD patient's whole blood

3.6. Expression of miR-98-5p in CAD patient's whole blood

miR-98 plays survival role in the myocardium by lowering oxidative stress and cell death of cardiomyocytes. miR-98-5p acts as cardioprotective modulator by reducing the apoptotic burden inthe cardiomyocytes. The expression of miR-98-5p was investigated by qRT-PCR. U6 was used as an endogenous control. miR-98-5p was significantly downregulated in CAD patient's blood. For statistical analysis, T test was performed by using GraphPad prism version 10.0.0. The graph was plotted in accordance with Mean ± SEM with significance (****) at $p<0.0001$ as shown in Figure 3.10.

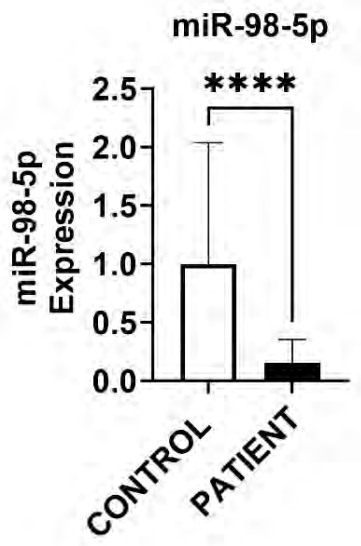

Figure 3.10 miR-98-5p expression analysis in MI patient's whole blood

3.7. Oxidative Stress Profile

3.7.1. Reactive oxygen species (ROS) Assay

ROS assay was performed to analyze oxidative profile in rat's tissue homogenate and serum samples. ROS activity was significantly upregulated in MI (isoproterenol) tissue homogenate and serum samples figure 3.11. For statistical analysis, T test was performed by usingGraphPad prism version 10.0.0. The graph was plotted in accordance with Mean ± SEM with significance (***) at $p<0.001$.

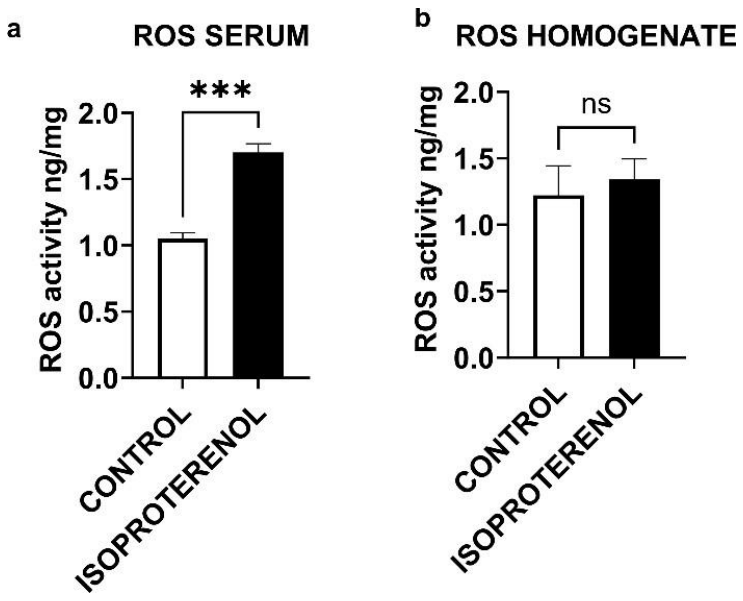

Figure 3.3.11. Oxidative profiling in animal model a. ROS activity in serum sample. b. ROS activity in tissue homogenate sample

3.7.1. Thiobarbituric acid Reactive substances (TBARs) level Assay

TBARs assay was performed to study oxidative profile in rat's tissue homogenate and serum samples. TBARs level was significantly upregulated in isoproterenol tissue homogenate and serum samples as compared to control. For statistical analysis, T test was performed by using GraphPad prism version 10.0.0. The graph was plotted in accordance with Mean ± SEM with significance (**) at $p<0.01$for serum sample and Mean ± SEM with significance (*) for at $p<0.05$ for tissue homogenate as shown in Figure 3.12.

3.8. Estimation of Antioxidative profile

3.8.1. Superoxide Dismutase (SOD) Assay

SOD enzyme acts as the first line of defense against oxidative stress. SOD activity was significantly downregulated in isoproterenol tissue homogenate and serum samples. For statistical analysis, T test was performed by using GraphPad prism version 10.0.0. The graph was plotted in accordancewith Mean ± SEM with significance (**) at $p<0.01$ for serum sample and Mean ± SEM with significance (*) for at $p<0.05$ for tissue homogenate as shown in Figure 3.13.

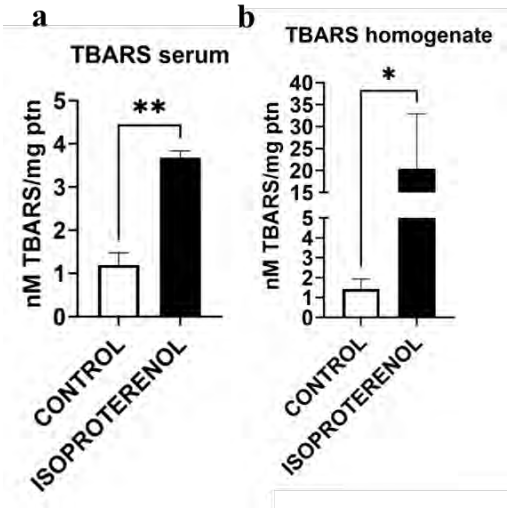

Figure 3.12 TBARs analysis in experimental model a. TBARs levels in serum samples of studied groups. b. TBARs levels in tissue homogenate sample of studied group.

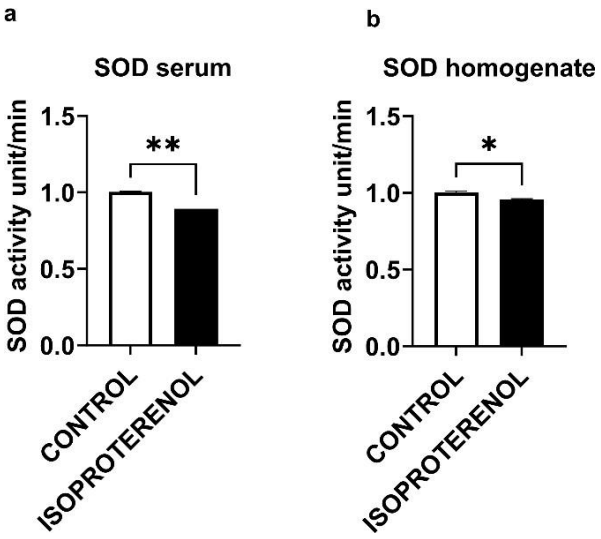

Figure 3.13 Graphical representation of SOD activity a. SOD activity in serum sample. b Graphical representation of SOD activity in tissue homogenate sample

3.8.2. Catalase Activity (CAT) Assay

CAT protects cardiomyocytes in oxidative stress condition. CAT reduces the burden of oxygen free radicals by converting hydrogen peroxide into water and oxygen. CAT activity was significantly downregulated in isoproterenol tissue homogenate and serum samples. For statistical analysis, T test was performed by using GraphPad prism version 10.0.0. The graph was plotted in accordance with Mean ± SEM with significance (**) at $p<0.01$ for serum sample and Mean ± SEM with significance for at (**) at $p<0.01$ for tissue homogenate as shown in Figure 3.14.

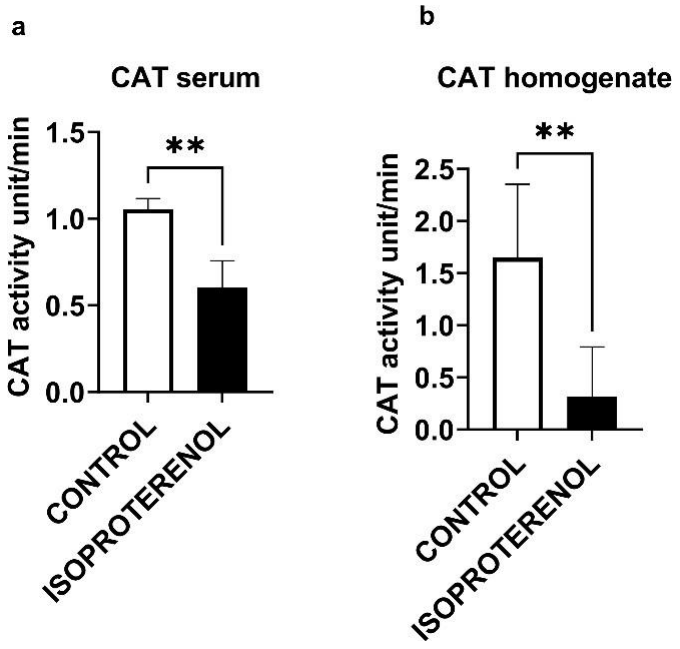

Figure 3.14 CAT activity of control and isoproterenol groups a serum b homogenate

3.8.3. Peroxidase (POD) Assay

POD plays regulatory in the degradation of reactive oxygen species. POD acts on hydrogen peroxide and converts it into water. POD activity was significantly downregulated in MI (isoproterenol) tissue homogenate and serum samples as compared to control. For statistical analysis, T test was performed by using GraphPad prism version 10.0.0. The graph wasplotted in accordance with Mean ± SEM with significance (**) at $p<0.01$for serum sample and Mean ± SEM with significance for at (**) at $p<0.01$ for tissue homogenate as shown in Figure 3.15.

3.8.4. Ascorbate Peroxidase Assay APX

APX uses ascorbate to convert hydrogen peroxide into water. Thus, acting as antioxidant defense enzyme. APX activity was significantly downregulated in MI (isoproterenol) tissue homogenate and serum samples. For statistical analysis, T test was performed by using GraphPad prism version 10.0.0. The graph was plotted in accordance with Mean ± SEM with significance (***) at p<0.001for serum sample and Mean ± SEM with significance (*) at p<0.05 for at for tissue homogenate as shown in Figure 3.16.

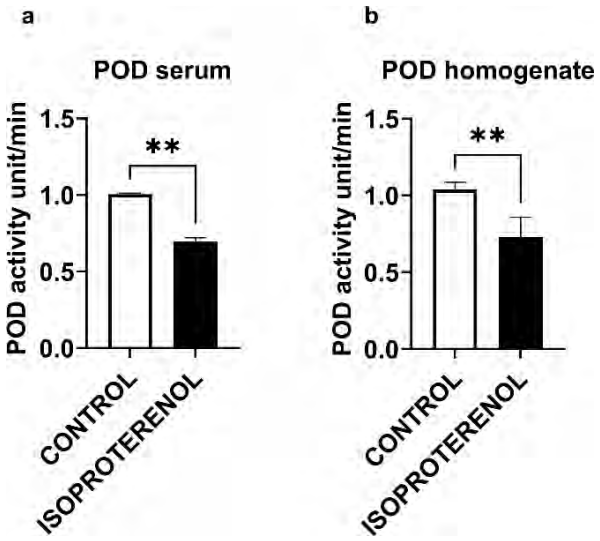

Figure 3.15 a. Graphic depiction of POD activity in serum. b Graphic depiction of POD activity in homogenate.

2.8.5. Reduced Glutathione Assay (GSH)

GSH degrades reactive oxygen species in normal physiological conditions. GSH activity was significantly downregulated in MI (isoproterenol) tissue homogenate and serum samples. For statistical analysis, T test was performed by using GraphPad prism version 10.0.0. The graph was plotted in accordance with Mean ± SEM with significance (*) at p<0.05 for serum sample and Mean ± SEM with significance (**) at p<0.01 for tissue homogenate as shown in Figure 3.17.

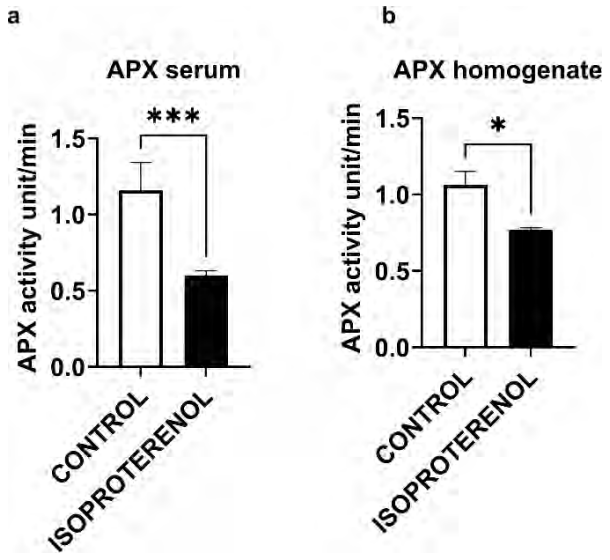

Figure 3.16 a APX activity in serum b APX activity in homogenate

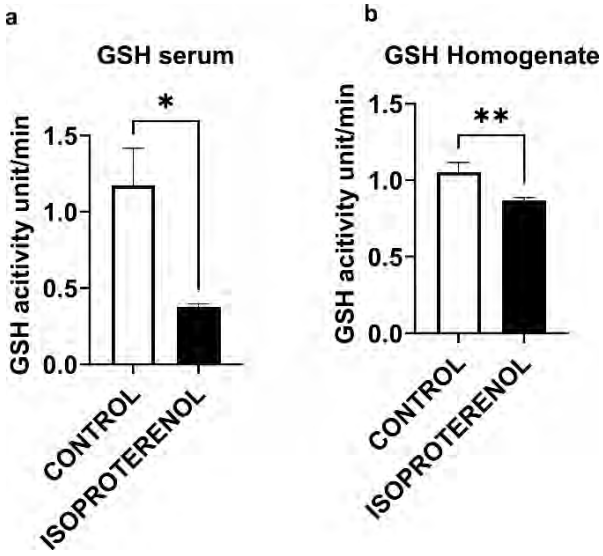

Figure 3.17 a. GSH activity in serum sample. b. GSH activity in tissue homogenate sample

3.9. Lipid profile and Liver Function Test

3.9.1. Cholesterol Assay

It is well known that cholesterol levels are highly increased in MI. Cholesterol assay was performed to study lipid profile using in samples. Using spectrophotometer (multiskan

GO, Thermo-Fischer scientific, USA), cholesterol levels of control and isoproterenol were measured by taking readings of absorbance at 500nm. Cholesterol level was significantly upregulated in MI (isoproterenol) treated serum samples. For statistical analysis, T test was performed by using GraphPad prism version 10.0.0. The graph was plotted in accordance with Mean ± SEM with significance (****) at p<0.00001 as shown in Figure 3.18.

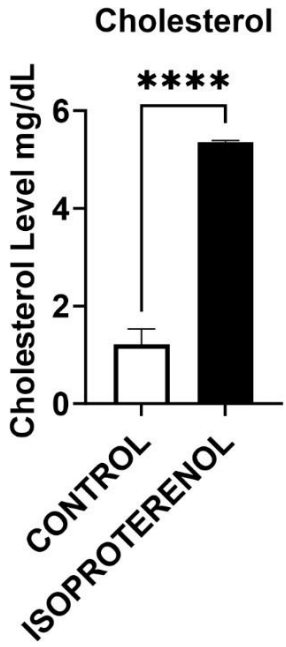

Figure 3.18 Cholesterol level in isoproterenol treated sample and control sample

3.9.2. Triglycerides

Triglyceride levels are upregulated in MI as reported in literature. Triglyceride level was significantly upregulated in MI (isoproterenol) treated serum samples. For statistical analysis, T test was performed by using GraphPad prism version 10.0.0. The graph was plotted in accordance with Mean ± SEM with significance (**) at p<0.01 for serum sample as shown in Figure 3.19.

3.9.3. Alanine Aminotransferase (ALT) Assay

ALT is a liver associated marker which is also released in high levels in case of MI. Therefore, it is widely studied that presence high levels of ALT in cardiac disorders including MI.

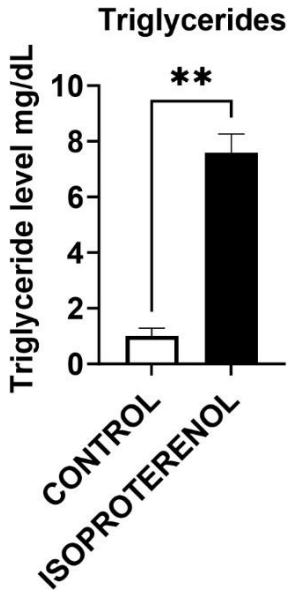

Figure 3.19 Triglyceride levels analysis in isoproterenol treated and control samples

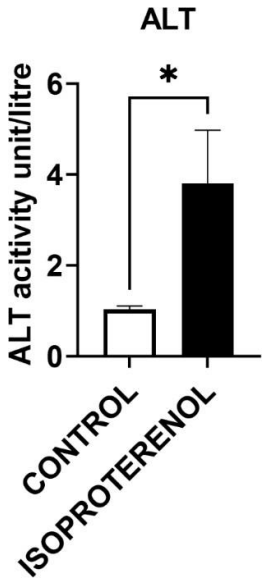

Figure 3.20 ALT activity in control and isoproterenol groups

Additionally, high ALT levels correspond to MI lead liver disorders. ALT activity was significantly upregulated in MI (isoproterenol) treated serumsamples. For statistical analysis, T test was performed by using GraphPad prism version 10.0.0.

The graph was plotted in accordance with Mean ± SEM with significance (*) at p<0.05 for serum as shown in Figure 3.20.

3.9.4. Aspartate Aminotransferase AST

Elevated AST levels in MI have been reported in various studies. AST is released into the blood during tissue damage i.e., MI and reaches liver. AST isliver associated cardiac biomarker in MI patients. AST activity was significantly upregulated in MI (isoproterenol) treated serum samples. For statistical analysis, T test was performed by using GraphPad prism version 10.0.0. The graph was plotted in accordance with Mean ± SEM with significance (***) at p<0.001 for serum as shown in Figure 3.21.

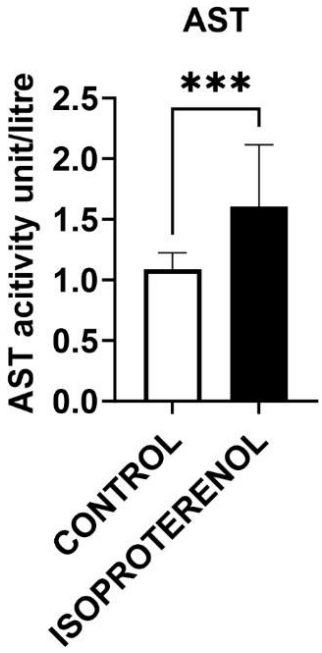

Figure 3.21 AST assay data showed higher AST activity in isoproterenol group as compared with control.

3.10. Protein Expression analysis of the apoptosis modulator

Western blot analysis was performed to identify the expression of protein in rat's samples.

3.10.1. Expression analysis of Bax

Bcl-2 associated X protein (Bax) is member of Bcl-2 which is pro-apoptotic agent. During MI, Bax levels are significantly elevated due to abnormally high rate of apoptosis. The expression of Bax in isoproterenol treated sample was significantly increased as compared to control sample. For statistical analysis, T test was performed by using GraphPad prism version 10.0.0. The graph was plotted in accordance with Mean ± SEM with significance (**) at $p<0.01$ for serum as shown in Figure 3.22.

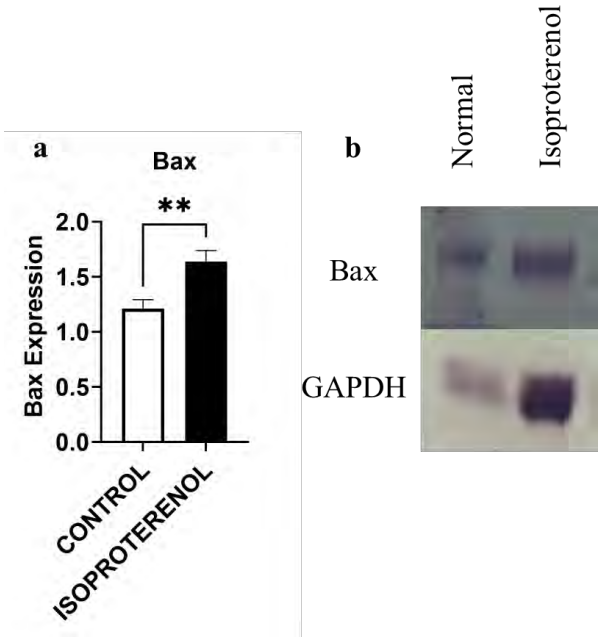

Figure 3.22. a. Graph of protein expression of Bax showed significant upregulation of Bax in isoproterenol group as compared to control. b. Blots image of BAX in control and isoproterenol group.

3.10.2. Expression analysis of Drp-1

Dynamin related protein-1 is a key player in the regulation of mitochondrial fission during mitophagy. Ischemic heart condition promotes high activation of Drp-1. High Drp-1 triggers apoptosis and ROS generation. The expression of Drp-1 in isoproterenol treated sample was significantly upregulated as compared to control sample. For statistical analysis, T test was performed by using GraphPad prism version 10.0.0. The graph was plotted in accordance with Mean ± SEM with significance (*) at $p<0.05$ for serum as shown in Figure. 3.23.

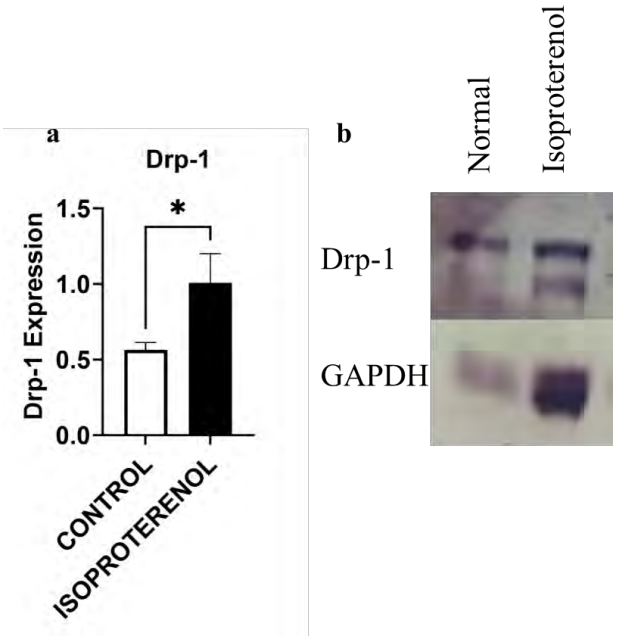

Figure 3.23 Western blot analysis showed upregulated expression of Drp-1 in isoproterenol induced rat group a. graphical representation of protein expression of Drp-1. b. Blots showing bands of Drp-1 in control and isoproterenol group.

3.10.3. Expression analysis of NFATc3

Nfat is a cardiac hypertrophic marker which plays crucial role in progression of cardiac hypertrophy. The expression of NFATc3 in isoproterenol treated sample was significantly downregulated as compared to control sample. For statistical analysis, T test was performed by using GraphPad prism version 10.0.0. The graph was plotted in accordance with Mean ± SEM with significance (***) at $p<0.001$ for serum as shown in Figure 3.24.

3.11. Expression of miR-15a in MI Rat's Tissue and Blood

In recent studies on animal model, it has been reported that miR-15a is highly expressed in MI. The expression of miR-15a in rat's tissue was investigated by qRT-PCR. U6 was used as an endogenous control. miR-15a was significantly upregulated in isoproterenol induced MI rat's tissue and blood. For statistical analysis, T test was performed by using GraphPad prism version 10.0.0. The graph was plotted in accordance with Mean ± SEM with significance (***) at $p<0.001$. Mean ± SEM with significance (*) at $p<0.05$ as shown in Figure 3.25 a and b.

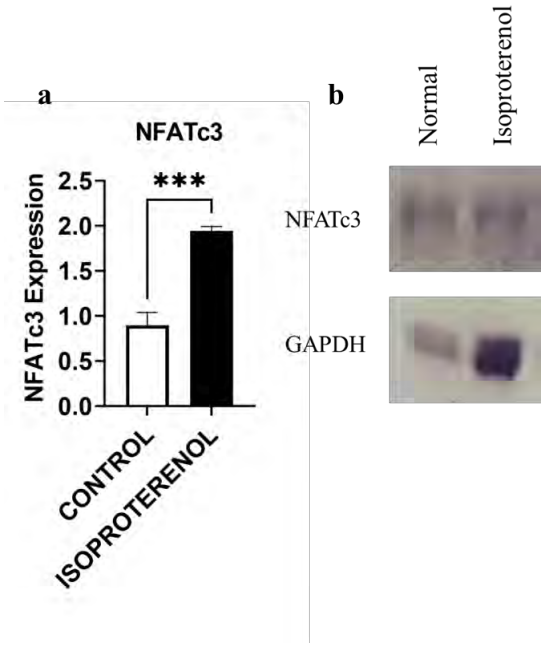

Figure 3.24. Expression of NFATc3 in control and isoproterenol rat group a. Graphs representing of protein expression of NFATc3. b. Blots presentation bands of NFATc3 in control and isoproterenol group.

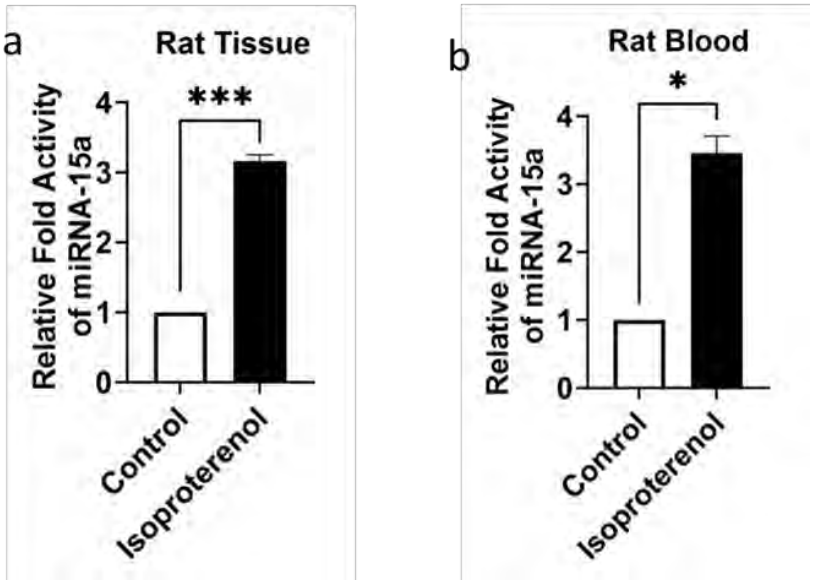

Figure 3.25. miR-15a expression analysis. a. Relative expression of miR-15a in Rat's tissue b. expression analysis in Rat Blood

3.12. Expression of miR-98-5p in MI Rat's tissue and Blood

Several studies on animal model show that the expression of miR-98-5p is downregulated in MI. The expression of miR-98-5p in rat's tissue was investigated by qRT-PCR. U6 was used as an endogenous control. miR-98-5p, was significantly upregulated isoproterenol induced MI rat's tissue and blood. For statistical analysis, T test was performed by using GraphPad prism version 10.0.0. The graph was plotted in accordance with Mean ± SEM with significance (***) at $p<0.001$ shown in Figure 3.26 a Mean ± SEM with significance (****) at $p<0.0001$ as shown in Figure 3.26 b.

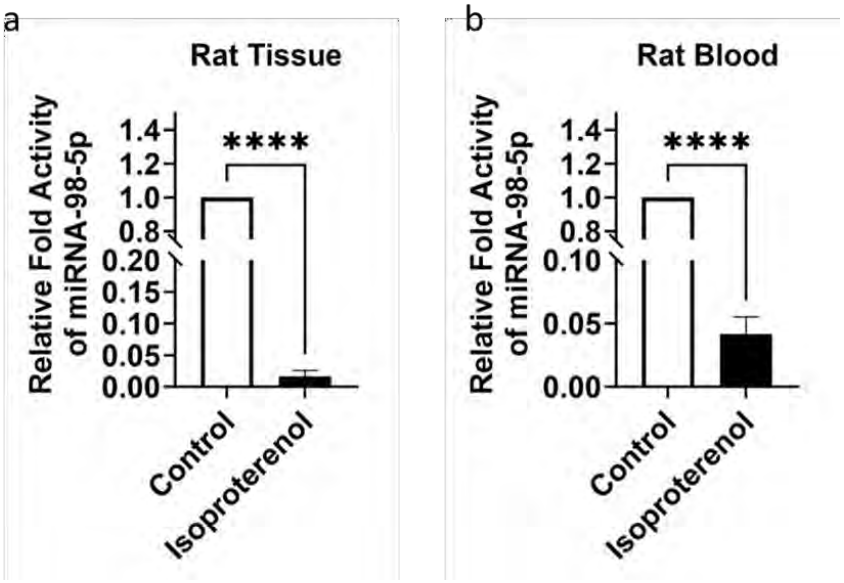

Figure 3.26 Expression analysis of miR-98-5p a. Rat's tissue b. Rat's blood

3.13. Protein expression analysis of ET-1

Endothelin -1 (ET-1) is potent vasoconstrictor as well as plays crucial role in the fibrosis in vascular tissues. ET-1 is also involved in the production of reactive oxygen species. In MI the expression of ET-1 is enhanced. Bioinformatics analysis showed ET-1 as putative target gene of miR-98-5p. In current study it was validated by introducing mimic of miR-98-5p. ET-1 is a direct target of miR98-5p. The expression of ET-1 was significantly increased in

isoproterenol group as compared to normal. With the treatment of miR-98-5p mimic, ET-1 expression declined significantly in comparison with isoproterenol group. One-way ANOVA was applied for the statistical analysis by using GraphPad prism version 10.0.0.

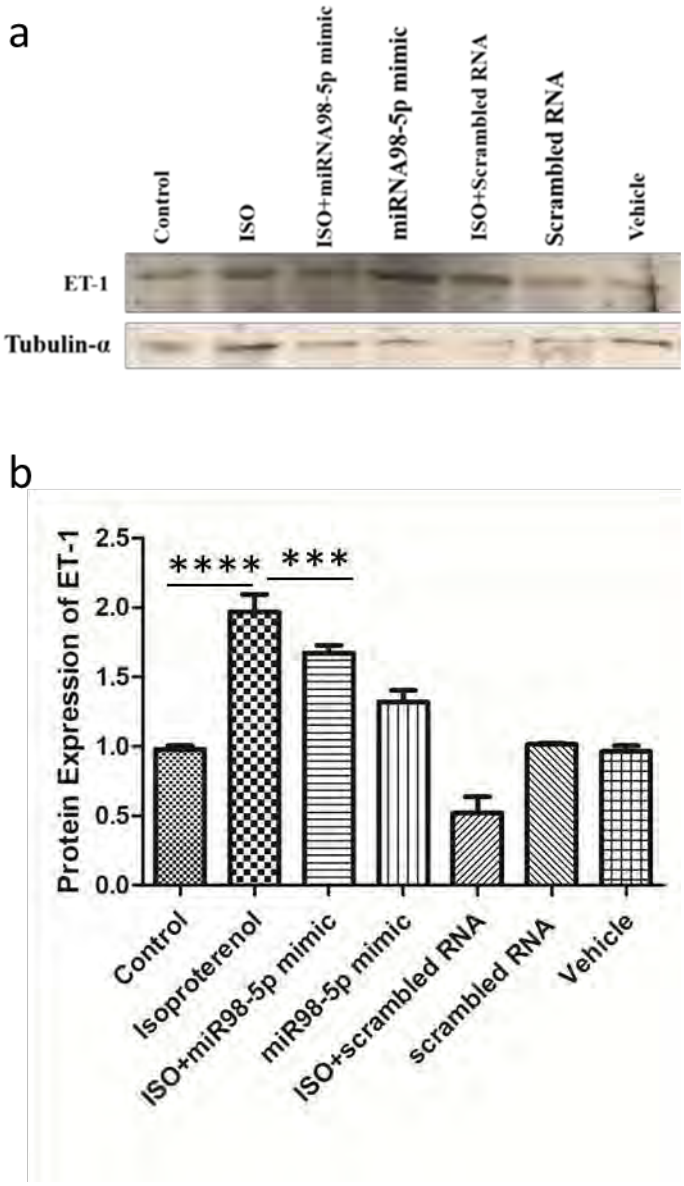

Figure 3.27 a. Analysis of protein expression of ET-1 in control, isoproterenol, and mimic of miR-98-5p. b. Graphical representation of ET-1 levels in control, isoproterenol and mimic miR-98-5ppus isoproterenol introduced groups.

The graph was plotted in accordance with Mean ± SEM with significance (****) at p<0.0001 for control and Isoproterenol group. Whereas as Mean ± SEM with significance (***) at p<0.001 for Isoproterenol and ISO+miR98-5p mimic group shown in Figure 3.27.

3.15. Histology

Histology slides were analyzed under microscope using Hematoxylin and Eosin staining as shown in figure. It has been demonstrated in various studies that in case of MI, apoptosis is enhanced, abrupt change in morphology of cells occurs and locality of nucleus changes. Total number of dead cells in isoproterenol group were significantly larger as compared to control group. Isoproterenol group showed significant change in morphology of cells in comparison with the control group. The cells were analyzed using SPOTCamw software.

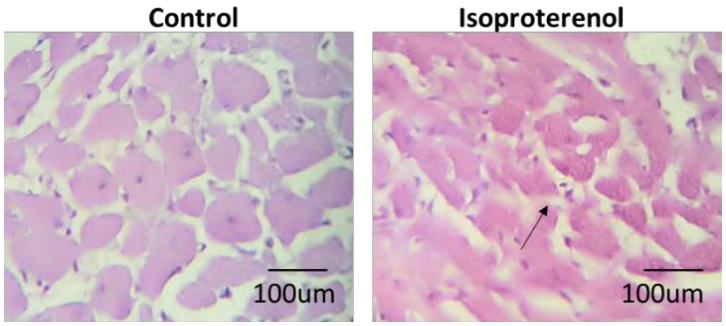

Figure 3.28 Hematoxylin and Eosin staining of control and isoproterenol for histopathological study.

4. Discussion

Myocardial infarction (MI) is caused by depletion of blood to the of myocardium. This deprivation of blood causes necrosis and apoptosis of cardiac cell death. Several different ischemic disorders also contribute to MI such as CAD (Ojha *et al*., 2021). Ischemic heart disease or MI is one of leading contributors of mortality across the globe (Khan *et al*., 2020). Furthermore, mortality rate in low- and middle-income countries is considerably greater as compared to high income countries (Yusuf *et al*., 2014). The mortality in developing countries is much higher becauseof lack of basic health facilities and awareness regarding risks of MI (Nascimento *et al*., 2019). The major risk factors of MI include tobacco consumption in the form of smoking, lipid disorders, diabetic history, and hypertension (Teo & Rafiq, 2021). The overall death rate of MI in men is more than women (Jayaraj *et al*., 2019). In current study, differential expression of miRNAs and their respective target genes in MI, was elucidated to propose the miRNA based diagnostic strategy. miRNAs were selected which were involved in different signaling pathways including inflammation and apoptosis. The MI model was developed to investigate the role of different miRNAs involved in *Bcl-2* signaling pathway. To further confirm the establishment of disease model, oxidative stress profiling, liver marker analysis and histological analysis were performed.

In current study, elevated levels of ROS (reactive oxygen species) and TBARs (thiobarbituric acid reactive substance assay) were observed in serum and homogenate samples of isoproterenol group as compared to control group. It is reported in a study on cardiomyopathy that TBARs levels are increased upon ISO administration (Hu *et al*.,2022). (Lee *et al*., 2022) reported that mitochondrial ROS levels are significantly increased upon isoproterenol induction. This implies that in MI cardiomyocytes undergo oxidative stress due to excessive production of ROS leading to increased TBARS accumulation.

In our study conducted on homogenate and serum samples of rat, the activities of antioxidant enzymes including SOD, POD, CAT and APX were found to be significantly reduced in isoproterenol group., Previously, the activities of SOD and CAT were reported to be

significantly decreased in isoproterenol group (Geng *et al*., 2015). Furthermore, another study confirmed that in patients of MI, SOD and catalase activities were significantly lesser than normal healthy control (Aladağ *et al*., 2021).Likewise in valvular heart disease patients, APX activity was found to be significantly lower in patient's group than healthy control group (Jan *et al*., 2022).

In current study, results of reduced glutathione (GSH) assay revealed significant decline in GSH activity in isoproterenol group of both serum and homogenate samples as compared to control. Previously, the enzymatic activity of GSH was reported to be reduced largely in isoproterenol group as compared with control group (Y. Yin *et al*, 2022).This confirms that activities of antioxidant enzymes in MI are low as compared with control group.

In our study, total cholesterol levels and triglyceride levels were measured. Total cholesterol levels and triglyceride levels in isoproterenol group were significantly higher as compared to the normal group. In a previous study on MI patients, it was reported that the cholesterol and triglycerides in serum samples of patients were significantly higher as compared to normal samples (Albrektsen *et al*., 2023).

In our study, AST and ALT levels were significantly higher in isoproterenol group as compared to normal group. Previously, abnormal levels of ALT and AST are well observed in myocardial infarction patients (Djakpo *et al*., 2020). A recent study deciphered that the levels of AST and ALT in patients of CAD risk was higher. In another study, elevated levels of AST and ALT were found out to be independent factor ofdeaths due to coronary artery disease (Xiaobo Liu & Liu, 2022). This indicates high releaseof serum transaminases to the liver after every cardiac cycle occurs in MI. The present study showed downregulation of ET-1 upon administering miR-98-5p mimic significantly downregulated ET-1 expression in comparison toisoproterenol group. (Wongtrakool *et al*., 2020) showed that upon treatment with mimic miR-98-5p the increased expression of ET-1 was significantly suppressed. This confirms that miR-98-5p may prove to be a promising diagnostic biomarker in MI.

In our study, miR-15a was upregulated in CAD patients than that of control. It is well studied that *Bcl-2* is a potential target of miR-15a. (Pekarsky *et al*., 2018). Our results

showed decreased expression of *Bcl-2* whereas the increased expression of miR-15a suggesting a correlation among them. This infers that survival role of *Bcl-2* is diminished in MI because of high expression of miR-15a. Our study showed similar resultsin Rat's tissue and blood sample in which expression of miR-15a was upregulated in isoproterenol group as compared to control.

In the present study, miR-98-5p expression was significantly downregulated in patient samples than that of control. Parallel to these findings, relative fold activity of miR-98- 5p in rat's blood and tissue sample was significantly downregulated. Previous study reported that during MI miR-98-5p is significantly downregulated (Sun *et al*., 2017). Moreover, it is experimentally studied that miR-98-5p expression is reduced in MI as compared to control group. (Wang *et al*., 2023). The bioinformatic analysis showed ET-1 as a putative target gene of miR-98-5p. In our experiment, high mRNA expression of ET-1 was observed in patients as compared to control samples. Experimental studies show that ET-1 is significantly upregulated in MI (Dąbek et al., 2022). This delineates that high ET-1 expression has major role in MI. The results of the ISO induced MI model also showed increased expression of ET-1. The increased expression of ET-1 and decreased expression of miR-98- 5p suggests the role of miR-98-5p in development and progression of MI.

The relative gene expression of Nfatc3 was significantly downregulated in isoproterenol as compared to control. Studies have shown that NFATc3 plays a regulatory role in inflammatory disorders (Pan *et al*., 2013). However, the specific expression of NFATc3 in MI blood samples is not studied well. We also performed western blotting to validate the protein expression of Bax, NFATc3, Drp-1 and Et-1 in ISO induced rats in comparison to control rats. In our study, the protein expression of Bax was significantly increased in isoproterenol group as compared to control group. It has been reported that infarct regions undergo apoptosis and necrosis at a very high rate (Lebeaupin *et al*., 2020). In a recent study the expression of Bax during MI was significantly high in response to increased induced apoptosis (Y. Yu *et al*., 2019). Our study showed significantly high protein expression of Drp-1 in isoproterenol group as that of control group. In a previous study, elevated expression of Drp-1 was observed in

MI model (W. Zhang *et al*., 2022). The protein expression of Nfatc3 was significantly upregulated in our isoproterenol. Nfatc3 is highly expressed during cardiac hypertrophy and MI (T. Wang *et al*., 2020).

Histological analysis of rat's heart tissues under light microscopy using Hematoxylin and Eosin staining showed increased percentage of dead cells in isoproterenol treated rat's sampleas that of control sample. The isoproterenol sample showed abnormal morphology of cardiaccells whereas in control sample cells with normal intact cell membranes were observed. It hasbeen studied that in MI normal cardiac morphology is disturbed. Intact cells are replaced with apoptotic cells due to high rate of apoptosis in MI (C. Yang *et al*., 2019). These results show that in MI, apoptotic signaling pathways are activated at an excessive rate ultimately leading to the death of cardiac cells.

The results of present study conclude that miRNAs show great potential in terms of diagnosisof MI by regulating *Bcl-2*. Aberrant expression of *Bcl-2*, Bax and Drp-1 in MI is related with apoptosis signaling cascade. Furthermore, biochemical analysis revealed characteristic features of MI pathophysiology in context of oxidative stress. The study delineates the comparison of changein expression of miRNAs with change of expression of their target genes in MI patients and isoproterenol group administered animal model. The differential expression of miRNAs and their respective target genes in CAD patients, may serve as a better diagnostic approach that will be beneficial for the diagnosis of MI.

5. REFERENCES

(US, N. A. P. (2010). Ischemic Heart Disease. *Institute of Medicine (US) Committee on Social Security Cardiovascular Disability Criteria: Updating the Social Security Listings.* doi:https://www.ncbi.nlm.nih.gov/books/NBK209964/

Ali, T., Shaheen, F., Mahmud, M., Waheed, H., Jan, M. I., Javed, Q., & Murtaza, I. (2015). Serotonin-promoted elevation of ROS levels may lead to cardiac pathologies in diabetic rat. *Arch Biol Sci, 67*(2), 655-661.

Ali, T., Waheed, H., Shaheen, F., Mahmud, M., Javed, Q., & Murtaza, I. (2015). Increased endogenous serotonin level in diabetic conditions may lead to cardiac valvulopathy via reactive oxygen species regulation. *Biologia, 70*(2), 273-278.

Aliska, G., Katar, Y., Mahata, L. E., Pratiwi, N., & Nuranisyah, V. (2022). Effect of Ramipril on Endothelin-1 Expression in Myocardial Tissue at Wistar Rats Induced Myocardial Infarction. *Open Access Macedonian Journal of Medical Sciences, 10*(A), 33-37.

Almaghrbi, H., Giordo, R., Pintus, G., & Zayed, H. (2023). Non-coding RNAs as biomarkers of myocardial infarction. *Clinica Chimica Acta*, 117222.

Álvarez-Álvarez, M. M., Zanetti, D., Carreras-Torres, R., Moral, P., & Athanasiadis, G. (2017). A survey of sub-Saharan gene flow into the Mediterranean at risk loci for coronary artery disease. *European Journal of Human Genetics, 25*(4), 472-476.

Batty, M., Bennett, M. R., & Yu, E. (2022). The role of oxidative stress in atherosclerosis. *Cells, 11*(23), 3843.

Budhram-Mahadeo, V., Fujita, R., Bitsi, S., Sicard, P., & Heads, R. (2014). Co-expression of POU4F2/Brn-3b with p53 may be important for controlling expression of pro-apoptotic genes in cardiomyocytes following ischaemic/hypoxic insults. *Cell Death & Disease, 5*(10), e1503-e1503.

Cai, J., Wang, X., Liao, W., Zhong, Y., Chen, L., & Zhang, Z. (2022). Silencing lncRNA 93358 Inhibits the Apoptosis of Myocardial Cells in Myocardial Infarction Rats by Inducing the Expression of SLC8A1.*BioMed Research International, 2022*, 1138709. doi:10.1155/2022/1138709

Cai, R., Gu, J., Sun, H., Liu, X., Mei, W., Qi, Y., . . . Cheng, J. (2015). Induction of SENP1 in myocardium contributes to abnormities of mitochondria and cardiomyopathy. *Journal of Molecular and Cellular Cardiology, 79*, 115-122. doi:https://doi.org/10.1016/j.yjmcc.2014.11.014

Carrington, E. M., Zhan, Y., Brady, J. L., Zhang, J.-G., Sutherland, R. M., Anstee, N. S., . . . Lew, A. M. (2017). Anti-apoptotic proteins *BCL-2*, MCL-1 and A1 summate collectively to maintain survival of immune cell populations both in vitro and in vivo. *Cell Death & Differentiation, 24*(5), 878-888. doi:10.1038/cdd.2017.30

CDC. (2022). About Multiple Cause of Death, 1999–2020. *Center for disease control and prevention*.

Chen, X., Ba, Y., Ma, L., Cai, X., Yin, Y., Wang, K., . . . Guo, X. (2008). Characterization of microRNAs in serum: a novel class of biomarkers for diagnosis of cancer and other diseases. *Cell research, 18*(10), 997-1006.

Cheng, C., Wang, Q., You, W., Chen, M., & Xia, J. (2014). MiRNAs as biomarkers of myocardial infarction: a meta-analysis. *PLoS One, 9*(2), e88566.

Chi, Y., Ma, Q., Ding, X.-Q., Qin, X., Wang, C., & Zhang, J. (2019). Research on protective mechanism of ibuprofen in myocardial ischemia-reperfusion injury in rats through the PI3K/Akt/mTOR signalingpathway. *European Review for Medical & Pharmacological Sciences, 23*(10).

Condrat, C. E., Thompson, D. C., Barbu, M. G., Bugnar, O. L., Boboc, A., Cretoiu, D., . . . Voinea, S. C. (2020). miRNAs as biomarkers in disease: latest findings regarding their role in diagnosis and prognosis. *Cells, 9*(2), 276.

Cruz, M. S., da Silva, A. M. G., de Souza, K. S. C., Luchessi, A. D., & Silbiger, V. N. (2020). miRNAs emerge as circulating biomarkers of post-myocardial infarction heart failure. *Heart Failure Reviews, 25*, 321-329.

Dąbek, J., Piotrkowicz, J., Głogowska-Ligus, J., Domagalska-Szopa, M., Szopa, A., & Schreiber, L. (2022). Expression of the Endothelin-1 Gene and Its Type a Receptor including Physical Activity among Patients with Acute Myocardial Infarction. *International Journal of Environmental Research and Public Health, 19*(12), 7289.

Dickstein, K. (2008). The Task Force for the diagnosis and treatment of acute and chronic heart failure 2008 of the European Society of Cardiology: Developed in collaboration with the Heart Failure Association of the ESC (HFA) and endorsed by the European Society of Intensive Care Medicine (ESICM). *Eur Heart J, 29*, 2388-2442.

Donia, T., & Khamis, A. (2021). Management of oxidative stress and inflammation in cardiovascular diseases: mechanisms and challenges. *Environmental Science and Pollution Research, 28*(26), 34121-34153.

Eitel, I., Nowak, M., Stehl, C., Adams, V., Fuernau, G., Hildebrand, L., . . . Thiele, H. (2010). Endothelin-1 release in acute myocardial infarction as a predictor of long-term prognosis and no-reflow assessed by contrast-enhanced magnetic resonance imaging. *American heart journal, 159*(5), 882-890.

Elkhader, B. A., Abdulla, A. A., & Omer, M. A. A. (2016). Correlation of smoking and myocardial infarction among sudanese male patients above 40 years of age. *Polish journal of radiology, 81*, 138.

F. (2021). Co-delivery of miRNA-15a and miRNA-16–1 using cationic PEGylated niosomes downregulates *BCL-2* and induces apoptosis in prostate cancer cells. *Biotechnology Letters, 43*, 981-994

Fan, J., & Watanabe, T. (2022). Atherosclerosis: Known and unknown. *Pathology International, 72*(3), 151-160.

Fan, K., Huang, W., Qi, H., Song, C., He, C., Liu, Y., . . . Sun, H. (2021). The Egr-1/miR-15a-5p/GPX4 axis regulates ferroptosis in acute myocardial infarction. *European Journal of Pharmacology, 909*, 174403.

Fan, P., Zhang, Y., Lu, Y.-T., Yang, K.-Q., Lu, P.-P., Zhang, Q.-Y., . . . Tian, T. (2021). Prognostic value of plasma big endothelin-1 in left ventricular non-compaction cardiomyopathy. *Heart, 107*(10), 836-841.

Fichtlscherer, S., De Rosa, S., Fox, H., Schwietz, T., Fischer, A., Liebetrau, C., . . . Müller-Ardogan, M. (2010). Circulating microRNAs in patients with coronary artery disease. *Circulation Research, 107*(5), 677-684.

Frangogiannis, N. G. (2011). Pathophysiology of myocardial infarction. *Comprehensive Physiology, 5*(4), 1841-1875.

Gao, C.-K., Liu, H., Cui, C.-J., Liang, Z.-G., Yao, H., & Tian, Y. (2016). Role of microRNA-195 in cardiomyocyte apoptosis induced by myocardial ischaemia–reperfusion injury. *Journal of genetics, 95*, 99-108.

Gao, L., & Jiang, F. (2016). MicroRNA (miRNA) profiling. *Cancer Gene Profiling: Methods and Protocols*, 151-161.

Ghaffari, M., Kalantar, S. M., Hemati, M., Dehghani Firoozabadi, A., Asri, A., Shams, A., . . . Haghiralsadat,

.

Glinge, C., Clauss, S., Boddum, K., Jabbari, R., Jabbari, J., Risgaard, B., . . . Wakili, R. (2017). Stability of circulating blood-based microRNAs–pre-analytic methodological considerations. *PLoS One, 12*(2),e0167969.

Harikrishnan, S., Jeemon, P., Mini, G., Thankappan, K., & Sylaja, P. (2018). GBD 2017 Causes of Death Collaborators. Global, regional, and national age-sex-specific mortality for 282 causes of death in 195 countries and territories, 1980-2017: a systematic analysis for the Global Burden of Disease Study 2017.

Hartley, A., Marshall, D. C., Salciccioli, J. D., Sikkel, M. B., Maruthappu, M., & Shalhoub, J. (2016). Trends in mortality from ischemic heart disease and cerebrovascular disease in Europe: 1980 to 2009. *Circulation, 133*(20), 1916-1926.

Haryono, A., Ramadhiani, R., Ryanto, G. R. T., & Emoto, N. (2022). Endothelin and the cardiovascular system: The long journey and where we are going. *Biology, 11*(5), 759.

Hayashi, I., Morishita, Y., Imai, K., Nakamura, M., Nakachi, K., & Hayashi, T. (2007). High-throughput spectrophotometric assay of reactive oxygen species in serum. *Mutation Research/Genetic Toxicology and Environmental Mutagenesis, 631*(1), 55-61.

Hermann, D. M., Xin, W., Bähr, M., Giebel, B., & Doeppner, T. R. (2022). Emerging roles of extracellular vesicle-associated non-coding RNAs in hypoxia: Insights from cancer, myocardial infarction and ischemic stroke. *Theranostics, 12*(13), 5776.

Hu, W.-S., Chen, T.-S., Cheang, K.-H., Liao, W.-Y., & Chang, C.-H. (2022). Mesenchymal Stem Cell Transplantation Increases Antioxidant Protein Expression and Ameliorates GP91/ROS/Inflammasome Signals in Diabetic Cardiomyopathy. *Journal of Cardiovascular Development and Disease, 9*(11), 381.

Hummel, M., Hantikainen, E., Adami, H.-O., Ye, W., Bellocco, R., Bonn, S. E., & Lagerros, Y. T. (2022). Association between total and leisure time physical activity and risk of myocardial infarction andstroke–a Swedish cohort study. *BMC Public Health, 22*(1), 1-15.

Jiang, S., & Yan, W. (2016). Current View of microRNA Processing. *Signal Transduction Insights, 5*, STI.S12317. doi:10.4137/STI.S12317

Joseph, P., Leong, D., McKee, M., Anand, S. S., Schwalm, J.-D., Teo, K., . . . Yusuf, S. (2017). Reducing the global burden of cardiovascular disease, part 1: the epidemiology and risk factors. *Circulation Research, 121*(6), 677-694.

Karim, S., Ishtiaq, A., & Murtaza, I. (2022). Mirnas as Potential Diagnostic Tool for Diabetes-Linked Myocardial Infarction. *American heart journal, 254*, 239-240.

Kumar, D., Pandit, R., & Yurdagul Jr, A. (2023). Mechanisms of continual efferocytosis by macrophages and its role in mitigating atherosclerosis. *Immunometabolism, 5*(1), e00017.

Lee, J. H., Kim, D. H., Kim, M., Jung, K. H., & Lee, K. H. (2022). Mitochondrial ROS-Mediated Metabolic and Cytotoxic Effects of Isoproterenol on Cardiomyocytes Are p53-Dependent and Reversed by Curcumin. *Molecules, 27*(4). doi:10.3390/molecules27041346

Li, Y., Cao, G.-y., Jing, W.-z., Liu, J., & Liu, M. (2023). Global trends and regional differences in incidence and mortality of cardiovascular disease, 1990− 2019: findings from 2019 global burden of diseasestudy. *European Journal of Preventive Cardiology, 30*(3), 276-286.

Liao, Z.-b., Tan, X.-l., Dong, K.-s., Zhang, H.-w., Chen, X.-p., Chu, L., & Zhang, B.-x. (2019). miRNA-448 inhibits cell growth by targeting *BCL-2* in hepatocellular carcinoma. *Digestive and Liver Disease, 51*(5), 703-711.

Lin, Y.-J., Juan, C.-C., Kwok, C.-F., Hsu, Y.-P., Shih, K.-C., Chen, C.-C., & Ho, L.-T. (2015). Endothelin-1
exacerbates development of hypertension and atherosclerosis in modest insulin resistant syndrome. *Biochemical and biophysical research communications, 460*(3), 497-503.

Liu, L.-F., Liang, Z., Lv, Z.-R., Liu, X.-H., Bai, J., Chen, J., . . . Wang, Y. (2012). MicroRNA-15a/b are up- regulated in response to myocardial ischemia/reperfusion injury. *Journal of geriatric cardiology: JGC, 9*(1), 28.

Lopez-Jimenez, F., Almahmeed, W., Bays, H., Cuevas, A., Di Angelantonio, E., le Roux, C. W., . . . Pinto, F.

J. (2022). Obesity and cardiovascular disease: mechanistic insights and management strategies. A joint position paper by the World Heart Federation and World Obesity Federation. *European Journal of Preventive Cardiology, 29*(17), 2218-2237.

Lopez, E. O., Ballard, B. D., & Jan, A. (2022). Cardiovascular disease *StatPearls [Internet]*: StatPearls Publishing.

Lyu, S.-q., Zhu, J., Wang, J., Wu, S., Zhang, H., Shao, X.-h., & Yang, Y.-m. (2023). Association between Plasma Big Endothelin-1 Level and The Severity of Coronary Artery Disease in Patients with Non- ST Segment-Elevated Myocardial Infarction. *Arquivos Brasileiros de Cardiologia, 120*, e20220294.

Mahjoob, G., Ahmadi, Y., Fatima rajani, H., Khanbabaei, N., & Abolhasani, S. (2022). Circulating microRNAs as predictive biomarkers of coronary artery diseases in type 2 diabetes patients. *Journal of ClinicalLaboratory Analysis, 36*(5), e24380.

Mechanic, O. J., Gavin, M., & Grossman, S. A. (2017). Acute myocardial infarction.

Minicucci, M. F., Azevedo, P. S., Polegato, B. F., Paiva, S. A., & Zornoff, L. A. (2011). Heart failure aftermyocardial infarction: clinical implications and treatment. *Clinical cardiology, 34*(7), 410-414.

Mohan, S. (2023). Public Health Policies for Prevention and Control of Cardiovascular Diseases *Public Health Approach to Cardiovascular Disease Prevention & Management* (pp. 135-143): CRC Press.

Moldoveanu, T. (2023). Apoptotic mitochondrial poration by a growing list of pore-forming BCL-2 family proteins. *Bioessays, 45*(3), 2200221.

Mons, U., Müezzinler, A., Gellert, C., Schöttker, B., Abnet, C. C., Bobak, M., . . . Kee, F. (2015). Impact of smoking and smoking cessation on cardiovascular events and mortality among older adults: meta- analysis of individual participant data from prospective cohort studies of the CHANCES consortium. *Bmj, 350*.

Mozaffarian, D., Benjamin, E., & AS, G. (2015). 3rd, Moy CS, Muntner P, Mussolino me, Nasir K, Neumar Rw, Nichol G, Palaniappan L, Pandey DK, Reeves MJ, Rodriguez CJ, Sorlie PD, Stein J, Towfighi a, Turan Tn, Virani SS, Willey JZ, Woo D, Yeh Rw, Turner MB. Heart disease and stroke statistics-2015 update: a report from the American Heart Association. *Circulation, 131*, e29-322.

Naito, S., Petersen, J., Sequeira-Gross, T., Zeller, T., Reichenspurner, H., & Girdauskas, E. (2022). Circulating microRNAs vs. aortic diameter in bicuspid aortic valve aortopathy. *Asian Cardiovascular and Thoracic Annals, 30*(8), 947-953.

National library of medicine, N. (2022). Acute Myocardial Infarction.

Ng, M. L., Ang, X., Yap, K. Y., Ng, J. J., Goh, E. C. H., Khoo, B. B. J., . . . Drum, C. L. (2023). Novel Oxidative

Stress Biomarkers with Risk Prognosis Values in Heart Failure. *Biomedicines, 11*(3), 917.

Nieves-Cintrón, M., Hirenallur-Shanthappa, D., Nygren, P. J., Hinke, S. A., Dell'Acqua, M. L., Langeberg, L. K., . . . Scott, J. D. (2016). AKAP150 participates in calcineurin/NFAT activation during the down- regulation of voltage-gated K+ currents in ventricular myocytes following myocardial infarction. *Cellular signalling, 28*(7), 733-740.

O'Brien, J., Hayder, H., Zayed, Y., & Peng, C. (2018). Overview of microRNA biogenesis, mechanisms of actions, and circulation. *Frontiers in endocrinology, 9*, 402.

O'Neill, K. L., Huang, K., Zhang, J., Chen, Y., & Luo, X. (2016). Inactivation of prosurvival *BCL-2* proteins activates Bax/Bak through the outer mitochondrial membrane. *Genes & development, 30*(8), 973-988.

Ojha, N., & Dhamoon, A. S. (2021). Myocardial infarction *StatPearls [Internet]*: StatPearls Publishing.

organization, W. h. (2022). WHO , Burden of noncommunicable diseases in Pakistan.

Ouyang, Z., & Wei, K. (2021). miRNA in cardiac development and regeneration. *Cell Regeneration, 10*(1), 1-21.

Pan, M.-G., Xiong, Y., & Chen, F. (2013). NFAT gene family in inflammation and cancer. *Current molecularmedicine, 13*(4), 543-554.

Gardarsdottir, H. R., Sigurdsson, M. I., Andersen, K., & Gudmundsdottir, I. J. (2022). Long-term survival of Icelandic women following acute myocardial infarction. *Scandinavian Cardiovascular Journal, 56*(1), 114-120.

Parmar, M. P., Kaur, M., Bhavanam, S., Mulaka, G. S. R., Ishfaq, L., Vempati, R., . . . Davalgi, S. (2023). A Systematic Review of the Effects of Smoking on the Cardiovascular System and General Health. *Cureus, 15*(4).

Pedrinelli, R., Ballo, P., Fiorentini, C., Denti, S., Galderisi, M., Ganau, A., . . . on behalf of the Gruppo di Studio Ipertensione e Cuore, S. I. d. C. (2012). Hypertension and acute myocardial infarction: an overview. *Journal of Cardiovascular Medicine, 13*(3), 194-202. doi:10.2459/JCM.0b013e3283511ee2

Perez, A. L., Grodin, J. L., Wu, Y., Hernandez, A. F., Butler, J., Metra, M., .. Armstrong, P. W. (2016). Increased mortality with elevated plasma endothelin-1 in acute heart failure: an ASCEND-HF biomarker substudy. *European Journal of Heart Failure, 18*(3), 290-297.

Qiao, Z., & Xu, Y. (2016). Salvianolic acid B alleviating myocardium injury in ischemia reperfusion rats.

African Journal of Traditional, Complementary and Alternative Medicines, 13(4), 157-161.

Rapsomaniki, E., Timmis, A., George, J., Pujades-Rodriguez, M., Shah, A. D., Denaxas, S., Smeeth, L. (2014). Blood pressure and incidence of twelve cardiovascular diseases: lifetime risks, healthy life-years lost, and age-specific associations in 1· 25 million people. *The Lancet, 383*(9932), 1899-1911.

Rotariu, D., Babes, E. E., Tit, D. M., Moisi, M., Bustea, C., Stoicescu, M., . Bungau, A. F. (2022). Oxidative

stress–complex pathological issues concerning the hallmark of cardiovascular and metabolic disorders. *Biomedicine & Pharmacotherapy, 152*, 113238.

Roth, G. A., Mensah, G. A., Johnson, C. O., Addolorato, G., Ammirati, E., Baddour, L. M., Benziger, C. P. (2020). Global burden of cardiovascular diseases and risk factors, 1990–2019: update from the GBD 2019 study. *Journal of the American College of Cardiology, 76*(25), 2982-3021.

Santovito, D., & Weber, C. (2022). Non-canonical features of microRNAs: Paradigms emerging from cardiovascular disease. *Nature Reviews Cardiology, 19*(9), 620-638.

Satam, H., Joshi, K., Mangrolia, U., Waghoo, S., Zaidi, G., Rawool, S., .. Das, G. (2023). Next-Generation Sequencing Technology: Current Trends and Advancements. *Biology, 12*(7), 997.

Schirmer, I., Bualeong, T., Budde, H., Cimiotti, D., Appukuttan, A., Klein, N., .. Meyer, R. (2018). Soluble adenylyl cyclase: A novel player in cardiac hypertrophy induced by isoprenaline or pressure overload. *PLoS One, 13*(2), e0192322.

Schlesinger, A. (2023). Heart Attack and Stroke *The Practice of Clinical Social Work in Healthcare* (pp. 151-174): Springer.

Shahjehan, R. D., & Bhutta, B. S. (2022). Coronary artery disease *StatPearls [Internet]*: StatPearls Publishing.

Sheikh, S. A. (2020). Role of plasma soluble lectin like oxidized low-density lipoprotein receptor-1 in severity of CAD patients and relationship with microRNA-98. *Med. J.*

Su, J., Li, J., Yu, Q., Wang, J., Li, X., Yang, J., Ji, L. (2020). Exosomal miRNAs as potential biomarkers for acute myocardial infarction. *IUBMB life, 72*(3), 384-400.

Sood, A., Singh, A., & Gadkari, C. (2023). Myocardial Infarction in Young Individuals: A Review Article. *Cureus, 15*(4).

Sucato, V., Coppola, G., Manno, G., Vadalà, G., Novo, G., Corrado, E., & Galassi, A. R. (2022). Coronary artery disease in South Asian patients: cardiovascular risk factors, pathogenesis and treatments. *Current Problems in Cardiology*, 101228.

Sun, C., Liu, H., Guo, J., Yu, Y., Yang, D., He, F., & Du, Z. (2017). MicroRNA-98 negatively regulates myocardial infarction-induced apoptosis by down-regulating Fas and caspase-3. *Scientific reports, 7*(1), 7460.

Tsai, N.-W., Chang, Y.-T., Huang, C.-R., Lin, Y.-J., Lin, W.-C., Cheng, B.-C., . . . Huang, C.-C. (2014). Association between oxidative stress and outcome in different subtypes of acute ischemic stroke. *BioMed research international, 2014*.

Tsao, C. W., Aday, A. W., Almarzooq, Z. I., Alonso, A., Beaton, A. Z., Bittencourt, M. S., . . . Commodore- Mensah, Y. (2022). Heart disease and stroke statistics—2022 update: a report from the American Heart Association. *Circulation, 145*(8), e153-e639.

Wang, Q., Liu, B., Wang, Y., Bai, B., Yu, T., & Chu, X. m. (2020). The biomarkers of key miRNAs and target genes associated with acute myocardial infarction. *PeerJ, 8*, e9129.

Wang, T., Zhai, M., Xu, S., Ponnusamy, M., Huang, Y., Liu, C.-Y., . . . Gao, X.-Q. (2020). NFATc3-dependent expression of miR-153-3p promotes mitochondrial fragmentation in cardiac hypertrophy by impairing mitofusin-1 expression. *Theranostics, 10*(2), 553.

Wei, S., Hu, S., Han, N., Wang, G., Chen, H., Yao, Q., . . . Sun, Q. (2023). Screening and evaluation of endogenous reference genes for miRNA expression analysis in forensic body fluid samples. *Forensic Science International: Genetics, 63*, 102827.

Wongtrakool, C., Ko, J., Jang, A. J., Grooms, K., Chang, S., Sylber, C., . . . Sutliff, R. L. (2020). MicroRNA-98 reduces nerve growth factor expression in nicotine-induced airway remodeling. *Journal of Biological Chemistry, 295*(52), 18051-18064.

Yang, X., Tang, X., Sun, P., Shi, Y., Liu, K., Hassan, S. H., . . . Yin, K.-J. (2017). MicroRNA-15a/16-1 antagomir ameliorates ischemic brain injury in experimental stroke. *Stroke, 48*(7), 1941-1947.

Yu, H., Cao, H., & Yu, H. (2023). MicroRNA-98 inhibition accelerates the development of atherosclerosis via regulation of dysfunction of endothelial cell. *Clinical and Experimental Hypertension, 45*(1), 2206068.

Zhai, C. L., Tang, G. M., Qian, G., Hu, H. L., Wang, S. J., Yin, D., & Zhang, S. (2019). MicroRNA-98 attenuates cardiac ischemia-reperfusion injury through inhibiting DAPK1 expression. *IUBMB life, 71*(2), 166- 176.

Zhang, J., Wang, Y.-J., Wang, X., Xu, L., Yang, X.-C., & Zhao, W.-S. (2019). PKC-mediated endothelin-1 expression in endothelial cell promotes macrophage activation in atherogenesis. *American Journal of Hypertension, 32*(9), 880-889.

Zhang, L., Zhang, Y., Zhao, Y., Wang, Y., Ding, H., Xue, S., & Li, P. (2018). Circulating miRNAs as biomarkers for early diagnosis of coronary artery disease. *Expert Opinion on Therapeutic Patents, 28*(8), 591-601.

Zhang, Q., Wang, L., Wang, S., Cheng, H., Xu, L., Pei, G., . . . He, C. (2022). Signaling pathways and targeted therapy for myocardial infarction. *Signal Transduction and Targeted Therapy, 7*(1), 78.